JOC The Journal of Organic Chemistry

pubs.acs.org/joc Article

Strongly Polarized π-Extended 1,4-Dihydropyrrolo[3,2-*b*]pyrroles Fused with Tetrazolo[1,5-*a*]quinolines

Mohammad B. Teimouri,* Irena Deperasińska, Matt Rammo, Marzena Banasiewicz, Charles W. Stark, Łukasz Dobrzycki, Michał K. Cyrański,* Aleksander Rebane,* and Daniel T. Gryko*

Cite This: *J. Org. Chem.* 2024, 89, 4657−4672 Read Online

ACCESS | Metrics & More | Article Recommendations | Supporting Information

ABSTRACT: A straightforward route to 1,4-dihydropyrrolo[3,2-*b*]pyrroles comprised of two electron-withdrawing quinoline or tetrazolo[1,5-*a*]quinoline scaffolds has been developed. The versatile multicomponent reaction affording 1,4-dihydropyrrolo[3,2-*b*]pyrroles combined with intramolecular direct arylation enables assembly of these products in just three steps from anilines with overall yields exceeding 30%. The planarized, ladder-type heteroacenes possess up to 14 conjugated rings. These nominally quadrupolar materials exhibit efficient fluorescence with wavelengths spanning most of the visible spectrum from green−yellow for the dyes possessing biaryl bridges and orange−red for the fully fused systems. In many cases, the fluorescence quantum yields are large, the solvatofluorochromic effects are strong, and the fluorescence is maintained even in crystalline state. Analysis of the electronic structure of these molecular architectures using quantum chemical methods suggests that the character and position of the flanking heterocycle determine the shape of HOMO and LUMO and their extension to *N*-aryl substituents, influencing the values of molar absorption coefficient. An experimental study of the two-photon absorption (2PA) properties has revealed that it occurs in the 700−800 nm range with apparent deviation from the Laporte parity selection rule, which may be attributed to Hertzberg−Teller contribution to vibronically allowed 2PA transition.

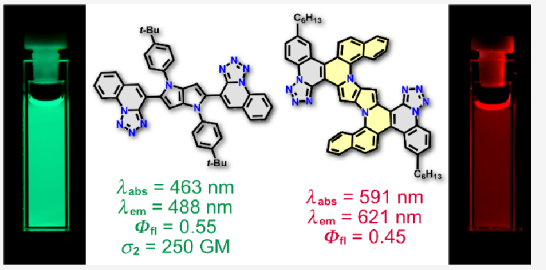

INTRODUCTION

Modern chemistry and materials science of complex conjugated functional dyes often implies controlled modulation of the optoelectronic properties achieved by fine-tuning the π-system. Extending the π-conjugation by linking two or more unsaturated hydrocarbons at the periphery of a conjugated architecture is a powerful method for targeted modification of the available π-cloud, leading to changes in the local or global delocalization character.[1] The π-electron distribution within a molecule can also be manipulated using both simple substituted aryl groups and exotic heteroaromatic motifs.[2]

The 1,4-dihydropyrrolo[3,2-*b*]pyrrole (DHPP) motif, comprised of two fused pyrrole units in a centrosymmetric orientation, is not only the strongest known electron donor among 10π-electron heteropentalenes but can also be obtained through an easily accessible one-pot synthesis.[3] The available facile synthesis of tetraaryl-1,4-dihydropyrrolo[3,2-*b*]pyrroles (TAPPs), combined with promising photophysical properties, is making TAPP scaffold-based organic chromophores attractive for many research applications.[4]

Over the past decade, the versatility of 1,4-dihydropyrrolo-[3,2-*b*]pyrroles has been demonstrated in an expansive range of areas of research including two-photon absorption (2PA),[5] ground- and excited-state symmetry breaking,[6] solvatofluorochromism,[7] tunable single-molecule conductance,[8] targeting the mitochondrial TET1 protein,[9] direct solvent probing via H-bonding interactions,[10] photochromic analysis of halocarbons,[11] high-performance organic field-effect transistors,[12] dye-sensitized solar cells,[13] and many others.[14−22]

The exceptional feature of DHPPs is that a convenient one-pot synthesis enables the assembly of the heterocyclic scaffold possessing four arenes linked via biaryl linkages.[23,24] The variety of these arenes is quite vast especially considering that by adding just one more synthetic step, e.g., direct arylation, the otherwise weakly coupled dye can be efficiently transformed into a fused planar compound possessing 8, 10, or 12 conjugated aromatic rings.[25] These advantages provide organic chemists a unique and versatile toolbox that currently has few if any analogs, at least in the area of centrosymmetric quadrupolar dyes.

Tetrazole is a five-membered, fully conjugated nitrogen-rich 6π-azaheterocycle consisting of a single carbon and four consecutive nitrogen atoms,[26] which render the system very electron deficient. Interestingly, tetrazole has the highest

Received: December 20, 2023
Revised: February 28, 2024
Accepted: March 11, 2024
Published: March 26, 2024

nitrogen content among the stable five-membered heterocycles. Despite the high nitrogen content, tetrazole and most of its derivatives remain relatively stable under the influence of heat or microwave radiation.[27] Furthermore, the related compounds are able to withstand a wide range of chemical environments such as strongly acidic and basic media, alkylating agents, dienophiles, as well as oxidizing and reducing conditions.[27] Even though tetrazoles[28] and their annulated derivatives have received considerable attention over the past years in fields of medicine, agriculture, and material science, it is still surprising that applications of tetrazoloquinoline-containing compounds as functional dyes have been rarely investigated to date.[29]

Our objective is to use unique features of TAPPs' chemistry for the synthesis of large, structurally unique, heavily *N*-doped nanographenes, possessing tetrazole scaffolds. We reasoned that incorporation of moderately electron-withdrawing moieties such as tetrazolo[1,5-*a*]quinoline and quinoline at strongly conjugated positions 2 and 5 can be utilized to endow resulting dyes with desired photophysical properties.

RESULTS AND DISCUSSION

Design and Synthesis. The synthesis of centrosymmetric quadrupolar TAPPs possessing fused tetrazole moieties starts from the preparation of the corresponding aldehyde. We were attracted by the exceptional simplicity of the Meth-Cohn synthesis of 2-chloro-3-formylquinolines, which enables the assembly of building blocks possessing the exact functionality required (in two steps from commercial arylamines).[30] The tetrazolo[1,5-*a*]quinolines precursors were obtained from the corresponding 2-chloroquinolines and NaN_3 via a general method involving the two-step process of S_NAr/ring−chain azido-tautomerization (see Supporting Information for details).[31]

Having 2-chloro-3-formylquinolines (**1a**−**e**) and tetrazolo-[1,5-*a*]quinoline-4-carbaldehyde (**5a**−**d**) in hand, we subjected them to our multicomponent reaction with primary aromatic amines **2a**−**f** and butane-2,3-dione (**3**), resulting in the formation of the corresponding 2,5-bis(2-chloroquinoline)-1,4-diaryl-pyrrolo[3,2-*b*]pyrroles (CQPPs) **4a**−**4l** and 2,5-bis(tetrazoloquinoline)-1,4-diaryl-pyrrolo[3,2-*b*]pyrroles (TQPPs) (**6a**−**6q**) in moderate to good yields (Schemes 1 and 2). Furthermore, the molecular structures of **4k** and **6j** were confirmed by X-ray crystallography (Figure 1b,c). The DHPP core in **4k** is perfectly planar, and the torsional angles between the peripheral substituted benzene rings attached to nitrogen atoms and DHPP core are 42° (Figure 1b). Chloroquinoline moieties attached to C-2 and C-5 atoms are both twisted at 51°. On the other hand, the dihedral angle between tetrazoloquinolinyl substituent and the DHPP core in **6j** is only 27° (Figure 1c). Noteworthy, this angle is only 35° for unsubstituted benzene in the ground state.[3,4]

Having a CQPP family with chlorine atoms and benzene rings strategically placed in respect to the central DHPP core in hand, precursors **4h**, **4i**, and **4l** were transformed in good yields into a ladder-type quinoline-fused pyrrolo[3,2-*b*]pyrroles (QFPPs) **10a**−**10c** utilizing double intramolecular direct arylation (Scheme 3). Unambiguous evidence for the proposed structure of **10** was finally obtained by single crystal X-ray diffraction analysis in the case of **10a** (Figure S3).

The analogous concept has been employed to obtain centrosymmetric, planarized tetrazoloquinoline-fused pyrrolo-[3,2-*b*]pyrroles (TQFPPs). The pivotal difference in these two

Scheme 1. Synthesis of 2,5-Bis(2-chloroquinoline)-1,4-diaryl pyrrolo[3,2-*b*]pyrroles (CQPPs)

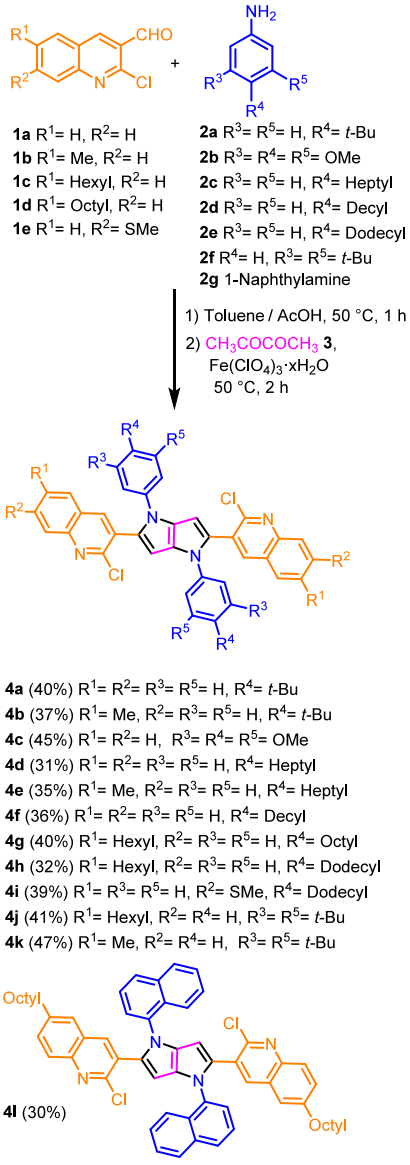

approaches is that in the case of quinoline-fused dyes, halogen atoms were placed on substituents at positions 2 and 5, whereas for tetrazoloquinoline-fused TAPPs, *N*-aryl substituents possessed bromine atoms. Dyes **6o** and **6p** were transformed into TQFPPs **11a** and **11b** via double intramolecular palladium-catalyzed direct arylation. High yields achieved for all these transformations encouraged us to attempt the synthesis of new TQFPPs incorporating [*n*]-helicenes with hope to obtain the molecules with interesting photophysical properties. To achieve this goal, the chosen building blocks were 1-amino-2-bromonaphthalene and 9-amino-10-bromophenanthrene as the arylamine components and tetrazolo[1,5-*a*]quinoline-4-carbaldehyde bearing hexyl or octyl substituents as the aldehyde. Consequently, the brominated TQPPs **6q** and **6r** were prepared using appropriate starting materials using our optimized three-component condensation (Scheme 4).

The 2-fold cyclization of TQPP **6q** was carried out to give the symmetric helicene **11c**, including four [4]azasubhelicenes and two [5]azasubhelicenes in 39% yield. When TQPP **6r** was

https://doi.org/10.1021/acs.joc.3c02916
J. Org. Chem. 2024, 89, 4657−4672

Scheme 2. Synthesis of 2,5-Bis(tetrazoloquinoline)-1,4-diaryl pyrrolo[3,2-*b*]pyrroles (TQPPs)

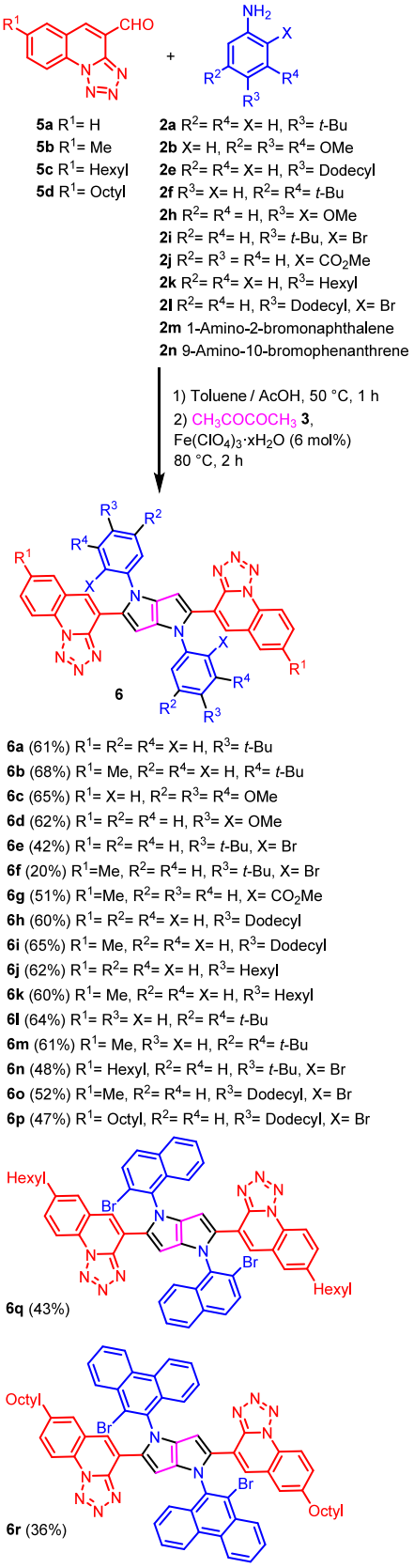

subjected to selective intramolecular direct arylation, to our surprise, the desired cyclization took place only on one side of the substrate, whereas debromination via a protodepalladation mechanism occurred on the other side, giving an unsymmetrical pyrrolopyrrole-containing triple azahelicene **11d** (Figure 1a) isolated in 26% yield (Scheme 4).

Photophysical Results. Spectroscopic properties of all prepared dyes were measured in toluene (if solubility allowed) (dielectric constant $\varepsilon = 2.38$) and dichloromethane (DCM, $\varepsilon = 8.93$). Spectroscopic properties of representative dyes **4a**, **4g**, **6a**, **6g**, **6r**, **10a**, **10c**, **11a**, **11c**, and **11d** are shown in Figures 2 and 3 and summarized in Table 1 (see Table S1 for comprehensive results). The absorption spectra of CQPPs (dyes **4a**−**4k**) are dominated by a strong band at around 390 nm, with the peak extinction coefficient values in the range $\varepsilon = 15000-30000\ M^{-1}\cdot cm^{-1}$. Comparison of the peak absorption wavelength of CQPPs with that of structurally related 2,5-bis(quinolin-2-yl)pyrrolo[3,2-*b*]pyrroles[25b] shows that in toluene the former dyes absorb wavelengths ca. 30−50 nm lower. This is attributed to the presence of chloro-substituent located *ortho*- to DHPP core, which, for steric reasons (confirmed by X-ray, Figure 1b), effectively disturbs ground state electronic coupling between the core and the periphery of the molecule. On the other hand, the absorption maxima of CQPPs are bathochromically shifted by ca. 30 nm compared to those of 2,5-bis(naphth-2-yl)pyrrolo[3,2-*b*]pyrroles,[24b] suggesting that the electron-withdrawing character of quinoline substituents is, nevertheless, clearly manifested. This behavior is even more pronounced for tetrazole-bearing TQPPs, which typically exhibit absorption maxima at 455−464 nm (dyes **6a**−**6q**), with a vibronic shoulder at ca. 20 nm lower. The only exception from this pattern is dye **6r**, for which the vibronic band is stronger than the origin band. The redshift observed for TQPPs was expected due to the significant increase in acceptor character of the substituents at positions 2 and 5 from weakly to strongly electron withdrawing. Additionally, the lack of an *ortho*-chloro substituent allows better planarization/electronic coupling in the ground state, which is confirmed by X-ray studies (Figure 1a). TQPPs also exhibit much higher extinction coefficients and fluorescence quantum yields (Φ_{fl}) than CQPPs, despite the presence of heavy atoms and nitrogen-rich aromatic rings, which often lead to very efficient intersystem crossing and quenching of fluorescence.[32]

Needless to say, rigid and planar QFPPs and **11a**−**c** display remarkably different characteristics compared to parent TAPP molecules. A significant ≈100 nm bathochromic shift of absorption were observed for dye **10a** (when compared to **4h**), as well as for dye **11a** (when compared to **6i**) (Figures 2 and 3). Further consequences of planarization were larger Φ_{fl} (reaching 100% in DCM in the case of dye **11a**) and smaller Stokes shifts observed for fused dyes, which are results of more restricted molecular motion comparing to the parent dyes. As expected, the properties of monocoupling product **11d** stand in the middle between those of substrates and the bis-coupled products.

As far as the solid-state emission is concerned, both groups of examined quadrupolar dyes, **4** and **6**, exhibit strikingly different properties. The analysis of solid-state spectra reveals that in the case of **4d**, **4h**, and **4i**, absorption is only slightly bathochromically shifted, i.e., to 425 nm, whereas emission is hypsochromically shifted (450−475 nm) compared to data collected in toluene. The only exception from this trend is found in the case of **4k** (λ_{em}^{max} = 515 nm), and it is presumably related to the presence of sterically encumbered substituents (four *tert*-butyl groups), which impact packing. On the other

https://doi.org/10.1021/acs.joc.3c02916
J. Org. Chem. 2024, 89, 4657−4672

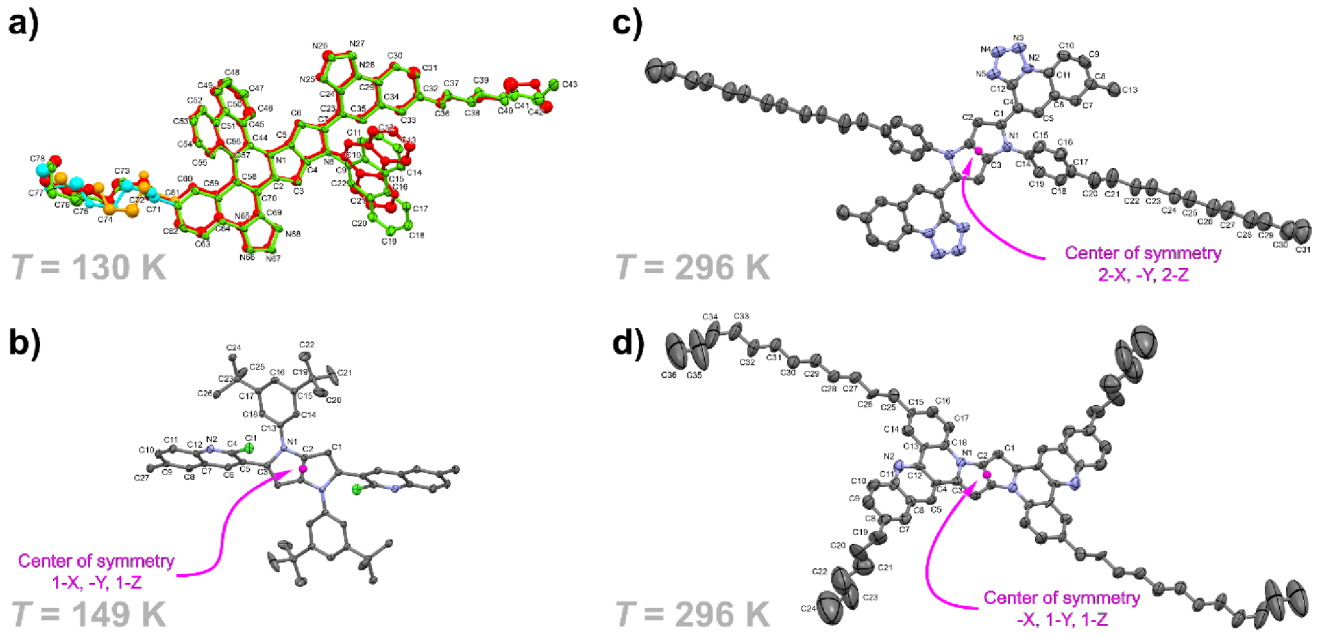

Figure 1. X-ray crystal structures of dyes **11d** (a), **4k** (b), **6j** (c), and **10a** (d). OTRTEP plot of molecules drawn at 50% probability level. Hydrogen molecules omitted for clarity.

hand, dyes **6a**, **6e**, **6i,** and **6o** do have bathochromically shifted both absorption and emission to 525 and 575 nm, respectively (see Supporting Information for details). For all these dyes, the fluorescence intensity is moderate ranging from 2.9% to 20%.

Two-Photon Absorption. Figure 4 presents the two-photon absorption (2PA) cross-section spectra in GM units (1 GM = 10^{-50} cm^4 s^{-1} photon) of representative dyes **4h**, **6h,** and **10a** in toluene measured with 120 fs laser pulses tuned in the wavelength range λ_{2PA}= 630−1040 nm (red line, lower horizontal scale) and through the fluorescence excitation method, which consists of scaling the reference-corrected 2PA spectral profiles according to absolute 2PA cross-section values determined at select wavelengths (black symbols). The linear absorption spectra of **4h**, **6h,** and **10a** in toluene are shown for comparison on a 2× expanded wavelength scale (blue line, upper horizontal axis).

In all three dyes, the 2PA shows distinct features with the maximum cross-section values, σ_{2PA} = 50 GM (770 nm) and 43 GM (660 nm) in **4h**, σ_{2PA} = 250 GM (775 nm) in **6h**, and σ_{2PA} = 5 GM (930 nm) and 25 GM (700 nm) in **10a**. The experimental observation that the TQPP **6h** shows almost 1 order of magnitude larger peak σ_{2PA} value compared to the CQPP and QFPP-type compounds correlates well with a stronger-acting electron-withdrawing ability of the attached tetrazole moiety. As a further testimony to the quadrupolar nature of these chromophores, none of the 2PA spectral profiles coincide with underlying 1PA transition profiles. Nevertheless, the ratio of σ_{2PA} vs ε_{1PA} (dashed black lines) remains finite even for the longest wavelength part of the spectra. Such apparent deviation from the Laporte parity selection rule has been previously observed for a number of nominally inversion-symmetric diketopyrrolopyrroles[33] and is most likely due to Hertzberg−Teller contribution to vibronically allowed 2PA transition.[22] It is worth to point out that much larger values of σ_{2PA} were reached for various strongly pyrrole derivatives bearing strongly polarized donor−acceptor structure.[34]

Computational Studies. DFT and TDDFT/M06/6-31G(d,p) calculations with the optimization of molecular structures in the ground electronic state S_0 and the lowest electronic excited state S_1 were performed for the description of the spectroscopic properties of molecules **4**, **6**, **10**, and **11** (for results, see Table 2). These dyes have been chosen since they constitute model dyes for the four groups of compounds studied in this project. The calculations also included the molecule **10-x**−regioisomer **10**, which is topologically similar to **11**. The M06 calculation method was chosen as it best reproduces the experimental results (Table S7 and Figure S7). Calculations were performed using the Gaussian 16 package.[35] The effect of solvent was described in the PCM procedure. The SOC elements were also calculated using the Orca program.[36]

Table 2 contains the calculated energies and oscillator strengths for the absorption ($S_0 \rightarrow S_1$) and fluorescence ($S_1 \rightarrow S_0$), characterizing structures optimized in the S_0 and S_1 states. Two of the considered molecules, **4** and **6**, are nonplanar systems. The angle between the planes of the peripheral arenes possessing electron-withdrawing character and the DHPP center in **4**, optimized in the S_0 ground state, is 43°, and is 20° in the case of compound **6**. In the S_1 excited state, the angle values slightly decrease to 32° and 18°, respectively. The planes between *N*-aryl substituents also form large angles with the DHPP plane: 43° and 45° in the S_0 and S_1 states of molecule **4**, and 48° and 49° in the case of **6**, respectively, which is corroborated by X-ray data (Figure 1).

The computational results, given in Table 2, capture the experimental facts, such as the red shifts of spectra of dye **6** relative to TAPP **4** and of dye **11** relative to TAPP **10** (i.e., in the context of the changing the acceptor), as well as **10** relative to **4** and **11** relative to **6** (i.e., in context fused vs nonfused system).

The calculations reveal that electronic transitions between the S_0 and S_1 states in all tested compounds are described by the electronic configuration {HOMO, LUMO}, where HOMO and LUMO have a specific structure, resembling "exciplex"

https://doi.org/10.1021/acs.joc.3c02916
J. Org. Chem. 2024, 89, 4657−4672

Scheme 3. Synthesis of Ladder-Type Quinoline-Fused Pyrrolo[3,2-*b*]pyrroles (QFPPs) via Intramolecular Double Direct Arylation

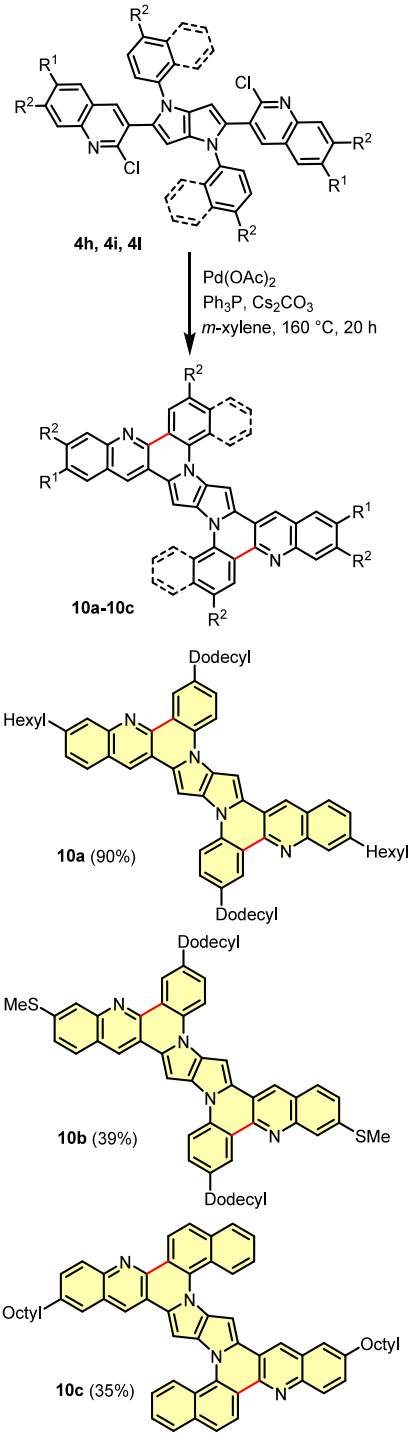

EDA systems. Meaning, the HOMO orbital is created from the HOMO of the DHPP donor with an admixture of HOMO orbitals of both acceptors, and the LUMO orbitals are created from a combination of LUMO orbitals of both acceptors with an admixture of the donor's LUMO orbital (see Figures 5 and S8; the orbitals of individual elements are shown in Table S8). Interestingly, formation of fully π-conjugated systems **10** and **11** is accompanied by spreading both HOMO and LUMO into *N*-aryl substituents (see Figure 5).

Therefore, the electronic transitions between the S_0 and S_1 states in all the tested compounds are qualitatively of the same nature: a multicenter CT transition with a charge shift between the central DHPP scaffold and two symmetrically arranged acceptor moieties at the periphery. Referring to the symbolic record of the CT transition energy $E_{CT} = I_D - E_A + E_{int}(D,A,R)$, it implies that the quantitative differences in the spectroscopic properties of these molecules are dictated by the interplay of several factors: differences in the electron affinity of acceptors and differences in interaction energy, resulting from variability in the mutual orientation of the donor and acceptors and the role played by the *N*-aryl substituents. The red shifts of the absorption and fluorescence spectra of **6** relative to **4** (and **11** relative to dye **10**) are in correspondence with the change in the electron affinity of the acceptor (≈1800 cm^{-1}, Table S8).

However, differences in the electron affinity of the acceptor are not the only reason for differences in spectroscopic properties of the tested molecules. In the case of such complex molecules, with the possibility of rotation of the components around the bonds connecting them, an important factor influencing the spectroscopic properties of these compounds is the mutual orientation of the planes of the individual elements. An interesting observation can be derived from probing the changes in the energy and the oscillator strength of the absorption depending on the mutual orientation of the donor and acceptors using compound **4** as an example (Figure 6). According to the results of the optimization of the molecular structure, the energy minimum for this compound corresponds to the geometry in which the angle between the planes of acceptors and donor is 43°. That means that in this geometry, a balance is achieved between the stabilizing role of interactions between donor and acceptors and the destabilizing role of steric interactions. This dye absorbs in DCM at 424 nm with an oscillator strength of 0.815 (Table 2). Both quantities change when moving away from equilibrium by changing the donor−acceptor angle (see Figure 6). In the case of orthogonality of the donor and acceptor planes (the system practically is not stabilized by the interactions between them), the absorption transition would be at higher energy at 418 nm with zero oscillator strength. In turn, in the planar case, the interaction of the donor with the acceptors is the strongest, which is reflected in the absorption at 460 nm with $f = 1.389$. The planar arrangement is destabilized by strong steric interactions (see the potential energy curve in Figure 6). Collectively, these results highlight that those attractive spectroscopic properties, such as low transition energy and high oscillator strength should emerge upon the formation of a fused system, i.e., **10**. The photophysical data gathered in Tables 1 and S7 corroborate this prediction.

The values of absorption energy and oscillator strength for compound **10** (Table 2) are close to those predicted based on calculations for the planarized version of **4** (Figure 6). This is not true, however, for the pair **6** and **11**. Despite the red shift of **11** relative to **6**, the oscillator strength of the transition between S_0 and S_1 in **11** is $f = 1.02$ and is smaller than the oscillator strength in **6** ($f = 1.79$). These computational predictions are fully corroborated by comparison of experimental molar absorption coefficients (Tables 1 and S7). Therefore, when creating a fused system, an additional circumstance appears that affects its spectroscopic properties.

The oscillator strength is a quantity strongly determined by the shape of the molecular orbitals. Therefore, the reasons for

https://doi.org/10.1021/acs.joc.3c02916
J. Org. Chem. 2024, 89, 4657−4672

Scheme 4. Synthesis of Pyrrolopyrrole-Containing Multiple Azahelicene 11a−11d via Intramolecular Palladium-Catalyzed Direct Arylation

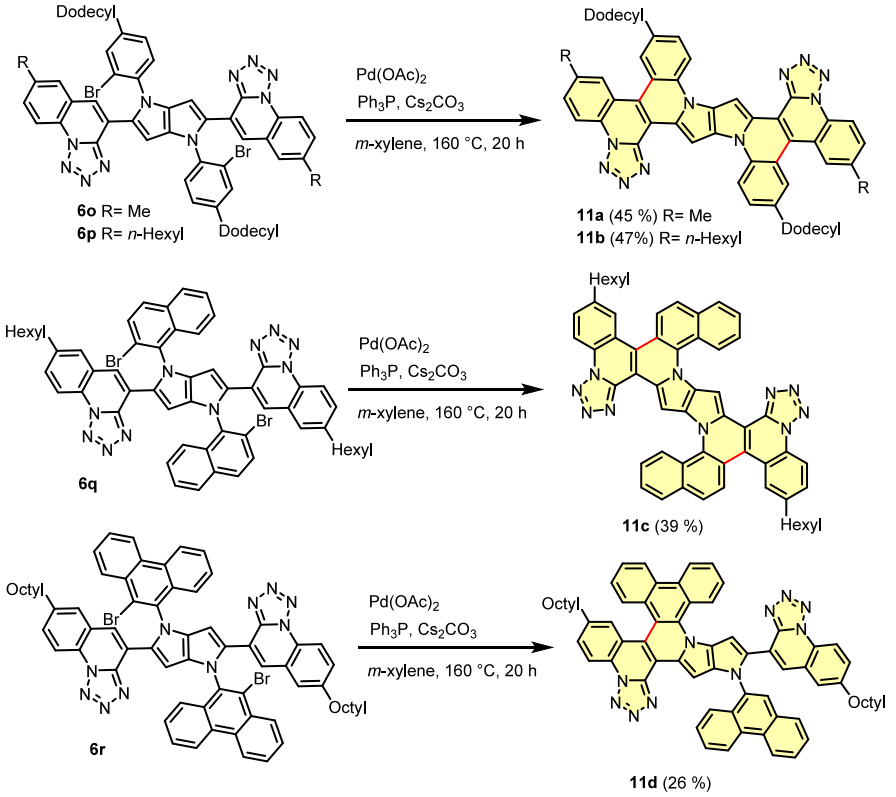

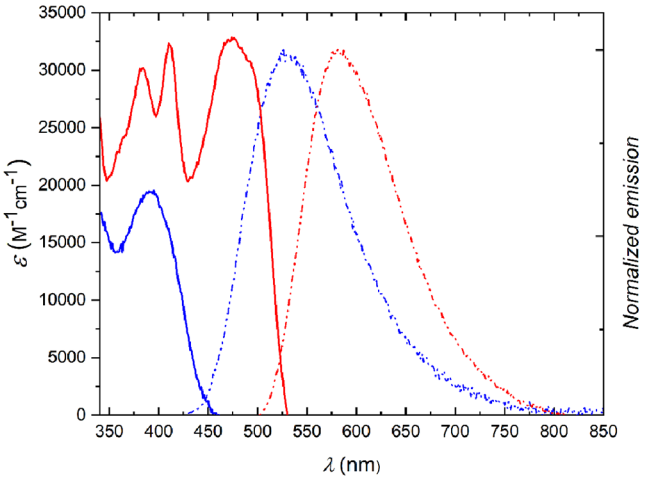

Figure 2. Molar extinction spectrum (solid line) and normalized fluorescence emission spectrum (dashed-dotted line) of compounds **4h** (blue) and **10a** (red) in DCM.

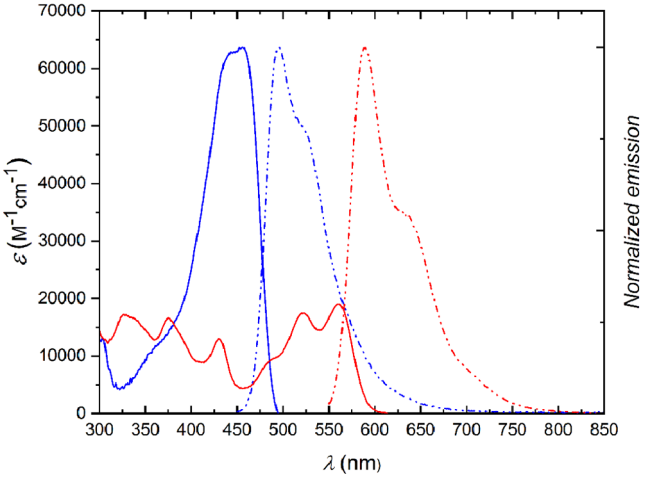

Figure 3. Molar extinction spectrum (solid line) and normalized fluorescence emission spectrum (dashed-dotted line) of compounds **6i** (blue) and **11a** (red) in DCM.

such discrepancies can be sought in differences in the extension of the charge distribution to atoms of moieties originating from electron-withdrawing moieties, which occurs in fused dyes. To confirm this, calculations were performed for the compound **10-x** (Figure 7), which is an isomer of **10** with a geometric structure analogous to **11** (for comparison of the both structures see Table S3).The calculated oscillator strength (f = 0.748) for fused system in geometry (**10-x**) is smaller than oscillator strength (f = 0.815) for nonfused molecule **4** and smaller than f = 1.203 for fused **10.** Therefore, the relationships between the transition energies and oscillator strengths of **10-x** and **4** are similar as the relations between **11** with **6** (see Table 2). Comparison of the orbitals **10** and **10-x** is given in Table S9 and indicates that the orbitals of **10-x** are more spread to the *N*-aryl substituents than the orbital of **10**.

CONCLUSIONS

We have provided experimental evidence that the efficient synthesis of quinoline derivatives enables not only preparation of 1,4-dihydropyrrrolo[3,2-*b*]pyrroles possessing planarized structures based on tetrazole but also previously inaccessible large planar *N*-doped nanographenes based on quinolines. The

https://doi.org/10.1021/acs.joc.3c02916
J. Org. Chem. 2024, 89, 4657−4672

Table 1. Spectroscopic Properties of Compounds 4a, 4g, 6a, 6g, 6r, 10a, 10c, 11a, 11c, and 11d Obtained in Toluene and DCM

	in DCM					in toluene				
entry	$\lambda_{max\ (Ab)}$ (nm)	$\varepsilon@\lambda_{max}$ (M^{-1} cm^{-1})	$\lambda_{max\ (Em)}$ (nm)	Stokes shift (cm^{-1})	Φ_{fl}	$\lambda_{max\ (Ab)}$ (nm)	$\varepsilon@\lambda_{max}$ ($M^{-1}cm^{-1}$)	$\lambda_{max\ (Em)}$ (nm)	Stokes shift (cm^{-1})	Φ_{fl}
4a	397	14700	540	6700	0.13	399	15100	480	4200	0.19
4g	390	20800	533	6900	0.15	398	19800	472	3900	0.19
6a	456	55400	495	1700	0.56	463	52100	488	1100	0.55
6g	458	58100	501	1900	0.55	459	-[a]	494	1500	0.51
6r	434	32500	486	2500	0.13	460	34600	480	900	0.16
10a	474	32800	581	3900	0.64	501	36900	532	1200	0.52
10c	483	31600	589	3700	0.26	485	33600	554	2600	0.49
11a	561	19100	590	900	1.0	563	40600	586	700	0.79
11c	590	13000	622	900	0.27	591	38100	621	800	0.45
11d	505	16600	611	3400	0.21	509	19700	591	2700	0.16

[a]Solubility was too low to reliably measure ε.

emission range of these prepared centrosymmetric, polarized TAPPs can be modulated from green to yellow, orange, and red, and their efficiency are typically moderate to high. Planarization of the chromophore structure results in considerable red shift of the emission wavelength (quinoline-derived dyes show strong yellow fluorescence and dyes possessing two tetrazoloquinoline units exhibit red emission). The two-photon absorption spectrum follows, in most cases, the Laporte rule, which is in accord with the inversion-symmetric structure, with the peak cross-section values reaching σ_{2PA} = 250 GM in the case of TAPP possessing two tetrazoloquinoline substituents at positions 2 and 5. Critically, subtle changes in geometry of these π-extended dyes have a profound effect on their photophysics. Computational studies suggest that intersystem crossing yield is responsible for variation for modulation of fluorescence intensity, thus confirming the notion that planarization of the geometry of polarized centrosymmetric dyes affords control over the molecular excited state. The change in the absorption strength between weakly coupled (biaryl bridges) and fused quadrupolar, centrosymmetric dyes is different for quinoline derivatives and for tetrazoloquinoline derivatives. In the latter case, the molar absorption coefficient actually decreases after planarization of the entire chromophore. The computational investigation enabled us to postulate that this striking difference has its origin in different orientation of the electron-deficient heterocyclic moiety, which causes the spread of the localization of both HOMO and LUMO on *N*-aryl moiety leading in turn to decrease in molar absorptivity. The relative position of singlet and triplet excited states plays a dominant role in determining the fate of the molecules after excitation. In particular, it is responsible for relatively small fluorescence quantum yield for bis(quinolinyl)dyes. Collectively, this work demonstrates that a tetrazole scaffold can be efficiently incorporated into the structure of quadrupolar, centrosymmetric functional dyes furnishing the latter with outstanding photophysical characteristics.

EXPERIMENTAL SECTION

General Information. All chemicals were bought from Sigma-Aldrich, TCI, Ambeed, and AlfaAesar and were used as received unless otherwise noted. All solvents used for reactions were analysis grade and were used without further purification. 2-Chloroquinoline-3-carbaldehyde derivatives **1**,[37] tetrazolo-[1,5-*a*]quinoline-4-carbaldehyde **5**,[38] 2-bromo-4-dodecylaniline,[39] and 9-amino-10-bromophenanthrene[40] were synthesized according to literature procedures. All reactions requiring heating were carried out using an oil bath. Reaction progress was monitored by thin layer chromatography (TLC), which was performed on aluminum foil plates, covered with Silica gel 60 F254 (Merck). The identity and purity of prepared compounds were proved by ^{1}H NMR and ^{13}C NMR spectroscopy, as well as by MS spectrometry (via APCI-MS or EI-MS). NMR spectra were measured on Varian 500 MHz and Varian 600 MHz instruments. Chemical shifts for ^{1}H NMR are expressed in parts per million (ppm) relative to tetramethylsilane (δ 0.00 ppm), $CDCl_3$ (δ 7.26 ppm), CD_2Cl_2 (δ 5.32 ppm), tetrachloroethane-[D_2] (δ 5.91 ppm), C_6D_6 (δ 7.16 ppm), and THF-[D_8] (δ 1.73 and 3.58 ppm). Chemical shifts for^{13}C NMR are expressed in ppm relative to $CDCl_3$ (δ 77.2 ppm), CD_2Cl_2 (δ 54.0 ppm), tetrachloroethane-[D_2] (δ 73.7 ppm), C_6D_6 (δ 128.4 ppm), and THF-[D_8] (δ 25.4 and 67.6 ppm). Data are reported as follows: chemical shift, multiplicity (s = singlet, d = doublet, dd = doublet of doublets, *t* = triplet, td = triplet of doublets, q = quartet, quint = quintet, sex = sextet, br. s = broad singlet, m = multiplet), coupling constant (in Hz), and integration. Because of the very low solubility of compounds **6a**, **6c**−**6e**, **6g**, and **10a**, their ^{13}C NMR spectra have been measured at high temperature in tetrachloroethane-[D_2]. Compounds **6f** and **10b** are not sufficiently soluble in common NMR solvents such as $CDCl_3$, acetone-[D_6], DMSO-[D_6], CD_3CN, methanol-[D_4], and tetrachloroethane-[D_2] (even after heating) to allow for measurement of ^{13}C NMR spectra.

All melting points for crystalline products were measured with automated melting point apparatus EZ-MELT and were given without correction.

Spectrophotometric grade solvents were used without further purification. All photophysical studies were performed with freshly prepared, air equilibrated solutions at room temperature. Steady-state fluorescence measurements were performed in standard 1 cm quartz cuvettes with dilute solutions (10^{-6} M, optical density <0.1) to minimize inner filter effects and/or aggregation. Absorption spectra were measured using a UV−vis Shimadzu UV-3600i Plus spectrophotometer. The calculation of molar absorption coefficient was conducted from Beer−Lambert's law equation. Emission spectra were measured using Edinburgh Instruments FS5 spectrofluorometer equipped with photomultiplier Hamamatsu R123456. Fluorescence quantum yields (Φ) were calculated from the equation:

https://doi.org/10.1021/acs.joc.3c02916
J. Org. Chem. 2024, 89, 4657−4672

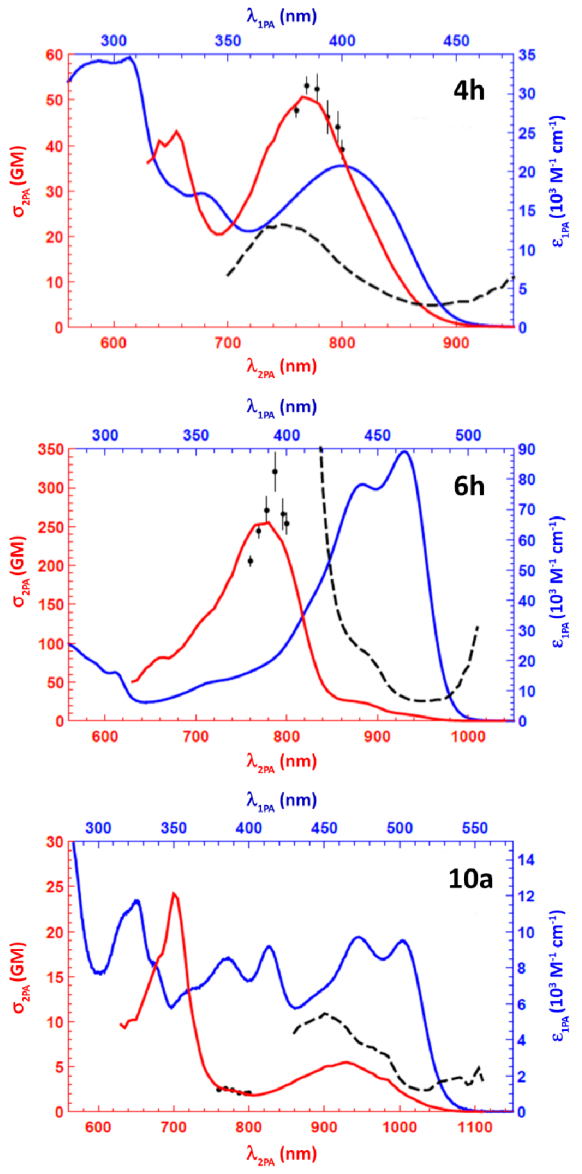

Figure 4. 2PA cross-section spectra of **4h**, **6h**, and **10a** in toluene solution in GM (red line, left vertical and lower horizontal scale). Black symbols—absolute 2PA cross sections measured at select wavelengths. Blue line—molar extinction spectra in toluene (blue line, upper horizontal axis). Dashed black line—ratio between the 2PA and 1PA spectral profiles (in arbitrary units).

$$\Phi = \Phi_{st} \cdot \frac{(1 - 10^{-A_{st}}) \cdot n^2 \cdot S}{(1 - 10^{-A}) \cdot n_{st}^2 \cdot S_{st}} \quad (1)$$

where A denotes absorbance, n is a refractive index of a solvent, and S is an integrated fluorescence intensity.

Typical Procedure for the Synthesis of 3,3′-(1,4-Bis(4-(*tert*-butyl)phenyl)-1,4-dihydropyrrolo[3,2-*b*]pyrrole-2,5-diyl)bis(2-chloroquinoline) (4a). Glacial acetic acid (2 mL), toluene (2 mL), 2-chloroquinoline-3-carbaldehyde (383 mg, 2 mmol, 2 equiv), and 4-(*tert*-butyl)aniline (299 mg, 2 mmol, 2 equiv) were placed in a 50 mL round-bottom flask equipped with a magnetic stir bar. The mixture reacted at 50 °C for 1 h. After that time, $Fe(ClO_4)_3 \cdot xH_2O$ (22 mg, 6 mol %) was added, followed by butane-2,3-dione (87 μL, 1 mmol, 1 equiv). The resulting mixture was stirred at 50 °C (oil bath) in an open flask under air for 2 h. Next, the heater was removed,

Table 2. TDDFT/M06/6-31G(d,p) Calculated Energies and Oscillator Strengths of the Absorption $S_0 \rightarrow S_i$ and Fluorescence $S_1 \rightarrow S_0$ Transitions

		absorption		fluorescence	
comp.	solvent	(nm)	*f*	(nm)	*f*
4	toluene	422	0.742	483	1.024
	DCM	424	0.815	492	1.289
6	toluene	471	1.706	531	1.930
	DCM	478	1.798	551	2.060
10	toluene	479	0.965	546	1.045
	DCM	489	1.203	563	1.286
11	toluene	550	0.849	642	0.876
	DCM	560	1.021	661	1.041
(**10-x**)	toluene	502	0.593	588	0.627
	DCM	510	0.748	603	0.783

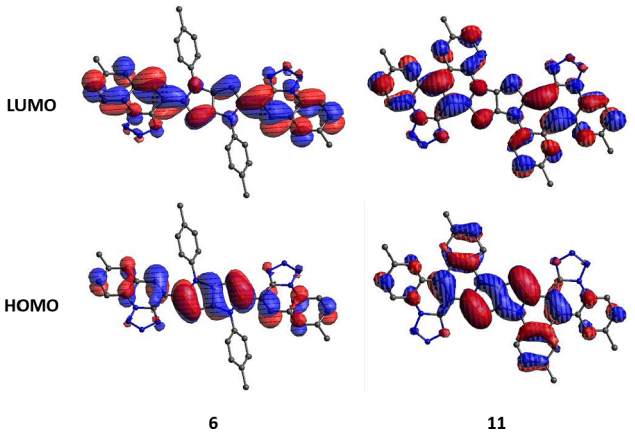

Figure 5. Shape of HOMO and LUMO orbitals of investigated dyes. Similarity and differences between HOMO and LUMO orbitals of nonfused and fused dyes, **6** and **11** − orbitals of **11** are spreading to *N*-aryl substituents.

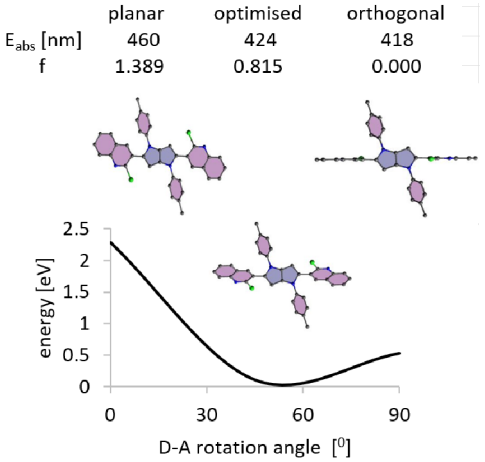

Figure 6. Potential energy curve of molecule **4** in S_0 state as a function of changes in the mutual orientation of the planes of the DHPP donor and acceptors. At the top, the absorption energy values together with the oscillator strengths, corresponding to the minimum geometry and extreme cases of coplanar and orthogonal donor and acceptor planes.

and 5 mL of methanol was added to the reaction mixture, and the resulting mixture was stirred for 10 min. The precipitate was filtered, washed with methanol (3 mL) and diethyl ether

https://doi.org/10.1021/acs.joc.3c02916
J. Org. Chem. 2024, 89, 4657−4672

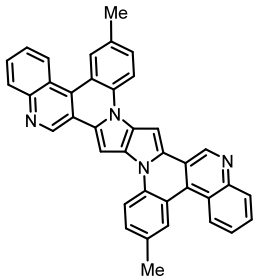

10-x

Figure 7. Structure of dye 10-x designed for computational purpose.

(5 mL), and recrystallized from a dichloromethane/hexane mixture and dried under vacuum affording 278 mg (40%) of pure product **4a** as a yellow solid.

The procedure for the synthesis of compounds **4b**−**4l** is similar to that of compound **4a**.

3,3′-(1,4-Bis(4-(tert-butyl)phenyl)-1,4-dihydropyrrolo[3,2-b]pyrrole-2,5-diyl)bis(2-chloroquinoline) (4a). Yellow solid (278 mg, 40%); m.p.: 333−334 °C; ^{1}H NMR (600 MHz, $CDCl_3$) δ 8.11 (d, J = 0.9 Hz, 2H), 8.03 (td, J = 8.8, 0.9 Hz, 2H), 7.74−7.70 (m, 4H), 7.55−7.52 (m, 2H), 7.28 (d, J = 9.0 Hz, 4H), 7.18 (d, J = 9.0 Hz, 4H), 6.59 (s, 2H), 1.26 (s, 18H); ^{13}C{^{1}H} NMR (151 MHz, $CDCl_3$) δ 150.5, 148.7, 146.4, 140.2, 136.9, 130.9, 130.6, 130.5, 128.2, 127.5, 127.5, 127.3, 126.8, 126.2, 123.7, 97.6, 34.5, 31.3; HRMS (APCI): m/z calculated for $C_{44}H_{39}Cl_2N_4$: 693.2552 [M + H]$^+$; found: 693.2549.

3,3′-(1,4-Bis(4-(tert-butyl)phenyl)-1,4-dihydropyrrolo[3,2-b]pyrrole-2,5-diyl)bis(2-chloro-6-methylquinoline) (4b). Yellow solid (267 mg, 37%); m.p.: 324−325 °C; ^{1}H NMR (600 MHz, $CDCl_3$) δ 8.02 (s, 2H), 7.90 (d, J = 8.6 Hz, 2H), 7.54 (dd, J = 8.6, 1.9 Hz, 2H), 7.47 (s, 2H), 7.27 (d, J = 8.7 Hz, 4H), 7.18 (d, J = 8.6 Hz, 4H), 6.57 (s, 2H), 2.50 (s, 6H), 1.26 (s, 18H); ^{13}C{^{1}H} NMR (151 MHz, $CDCl_3$) δ 149.6, 148.6, 145.2, 139.6, 137.3, 137.0, 132.7, 130.8, 130.8, 127.9, 127.4, 126.9, 126.3, 126.2, 123.6, 97.5, 34.4, 31.3, 21.6; HRMS (APCI): m/z calculated for $C_{46}H_{43}Cl_2N_4$: 721.2859 [M + H]$^+$; found: 721.2862.

3,3′-(1,4-Bis(3,4,5-trimethoxyphenyl)-1,4-dihydropyrrolo-[3,2-b]pyrrole-2,5-diyl)bis(2-chloroquinoline) (4c). Yellow solid (343 mg, 45%); m.p.: 330−331 °C; ^{1}H NMR (600 MHz, $CDCl_3$) δ 8.14 (s, 2H), 8.04 (d, J = 8.6 Hz, 2H), 7.76−7.73 (m, 4H), 7.57 (t, J = 7.5 Hz, 2H), 6.60 (s, 2H), 6.50 (s, 4H), 3.80 (s, 6H), 3.58 (s, 12H); ^{13}C{^{1}H} NMR (126 MHz, $CDCl_3$) δ 153.5, 150.6, 146.6, 140.3, 136.1, 135.1, 130.9, 130.9, 130.4, 128.3, 127.5, 127.5, 127.4, 126.6, 101.9, 97.4, 61.0, 56.1; HRMS (APCI): m/z calculated for $C_{42}H_{35}Cl_2N_4O_6$: 761.1934 [M + H]$^+$; found: 761.1932.

3,3′-(1,4-Bis(4-heptylphenyl)-1,4-dihydropyrrolo[3,2-b]-pyrrole-2,5-diyl)bis(2-chloroquinoline) (4d). Off-white solid (241 mg, 31%); m.p.: 206−207 °C; ^{1}H NMR (500 MHz, $CDCl_3$) δ 8.09 (s, 2H), 8.04 (d, J = 8.5 Hz, 2H), 7.73−7.70 (m, 4H), 7.54 (t, J = 7.5 Hz, 2H), 7.17 (d, J = 8.0 Hz, 4H), 7.08 (d, J = 8.0 Hz, 4H), 6.61 (s, 2H), 2.54 (t, J = 7.8 Hz, 4H), 1.59−1.53 (m, 4H), 1.30−1.22 (m, 16H), 0.87 (t, J = 6.9 Hz, 6H); ^{13}C{^{1}H} NMR (126 MHz, $CDCl_3$) δ 150.4, 146.4, 140.7, 140.2, 137.1, 130.9, 130.7, 130.5, 129.2, 128.2, 127.5, 127.4, 127.3, 126.8, 124.1, 97.5, 35.4, 31.8, 31.2, 29.2, 29.1, 22.6, 14.1; HRMS (APCI): m/z calculated for $C_{50}H_{51}Cl_2N_4$: 777.3491 [M + H]$^+$; found: 777.3497.

3,3′-(1,4-Bis(4-heptylphenyl)-1,4-dihydropyrrolo[3,2-b]-pyrrole-2,5-diyl)bis(2-chloro-6-methylquinoline) (4e). Off-white solid (282 mg, 35%); m.p.: 253−254 °C; ^{1}H NMR (600 MHz, $CDCl_3$) δ 7.99 (s, 2H), 7.93 (d, J = 8.6 Hz, 2H), 7.55 (dd, J = 8.6, 1.9 Hz, 2H), 7.46 (s, 2H), 7.17 (d, J = 8.1 Hz, 4H), 7.08 (d, J = 8.1 Hz, 4H), 6.59 (s, 2H), 2.54 (t, J = 7.8 Hz, 4H), 2.51 (s, 6H), 1.58−1.55 (m, 4H), 1.30−1.23 (m, 16H), 0.86 (t, J = 6.8 Hz, 6H); ^{13}C{^{1}H} NMR (126 MHz, $CDCl_3$) δ 149.5, 145.0, 140.6, 139.7, 137.4, 137.1, 132.8, 130.8, 130.8, 129.2, 127.8, 127.3, 126.8, 126.3, 124.1, 97.4, 35.4, 31.8, 31.2, 29.2, 29.1, 22.6, 21.6, 14.1; HRMS (APCI): m/z calculated for $C_{52}H_{55}Cl_2N_4$: 805.3804 [M + H]$^+$; found: 805.3807.

3,3′-(1,4-Bis(4-decylphenyl)-1,4-dihydropyrrolo[3,2-b]-pyrrole-2,5-diyl)bis(2-chloroquinoline) (4f). Off-white solid (311 mg, 36%); m.p.: 203−204 °C; ^{1}H NMR (500 MHz, $CDCl_3$) δ 8.08 (s, 2H), 8.02 (d, J = 8.2 Hz, 2H), 7.73−7.70 (m, 4H), 7.54 (t, J = 7.4 Hz, 2H), 7.17 (d, J = 8.0 Hz, 4H), 7.08 (d, J = 8.0 Hz, 4H), 6.61 (s, 2H), 2.54 (t, J = 7.8 Hz, 4H), 1.59−1.53 (m, 4H), 1.30−1.24 (m, 28H), 0.87 (t, J = 6.8 Hz, 6H); ^{13}C{^{1}H} NMR (126 MHz, $CDCl_3$) δ 150.5, 146.5, 140.6, 140.2, 137.1, 130.9, 130.7, 130.5, 129.2, 128.3, 127.5, 127.4, 127.2, 126.8, 124.1, 97.4, 35.4, 31.9, 31.2, 29.6, 29.6, 29.5, 29.3, 29.3, 22.7, 14.1; HRMS (APCI): m/z calculated for $C_{56}H_{63}Cl_2N_4$: 861.4430 [M + H]$^+$; found: 861.4433.

3,3′-(1,4-Bis(4-octylphenyl)-1,4-dihydropyrrolo[3,2-b]-pyrrole-2,5-diyl)bis(2-chloro-6-hexylquinoline) (4g). Yellow solid (390 mg, 40%); m.p.: 121−122 °C; ^{1}H NMR (500 MHz, $CDCl_3$) δ 8.02 (s, 2H), 7.91 (d, J = 8.6 Hz, 2H), 7.56 (dd, J = 8.7, 2.0 Hz, 2H), 7.46 (d, J = 1.9 Hz, 2H), 7.17 (d, J = 8.2 Hz, 4H), 7.08 (d, J = 8.1 Hz, 4H), 6.58 (s, 2H), 2.76 (t, J = 7.8 Hz, 4H), 2.54 (t, J = 7.8 Hz, 4H), 1.60−1.53 (m, 4H), 1.71−1.66 (m, 4H), 1.37−1.24 (m, 32H), 0.91−0.85 (m, 12H); ^{13}C{^{1}H} NMR (126 MHz, $CDCl_3$) δ 149.6, 145.4, 142.2, 140.5, 139.7, 137.2, 132.0, 130.9, 130.8, 129.2, 128.0, 127.3, 126.8, 125.7, 124.0, 97.3, 35.9, 35.4, 31.9, 31.7, 31.2, 31.1, 29.4, 29.3, 29.2, 29.0, 22.6 (2 signals), 14.1 (2 signals); HRMS (APCI): m/z calculated for $C_{64}H_{79}Cl_2N_4$: 973.5682 [M + H]$^+$; found: 973.5696.

3,3′-(1,4-Bis(4-octylphenyl)-1,4-dihydropyrrolo[3,2-b]-pyrrole-2,5-diyl)bis(2-chloro-6-hexylquinoline) (4h). Pale yellow solid (348 mg, 32%); m.p.: 108−109 °C; ^{1}H NMR (600 MHz, $CDCl_3$) δ 8.01 (s, 2H), 7.91 (d, J = 8.6 Hz, 2H), 7.55 (d, J = 8.6 Hz, 2H), 7.45 (s, 2H), 7.16 (d, J = 7.9 Hz, 4H), 7.06 (d, J = 7.9 Hz, 4H), 6.57 (s, 2H), 2.75 (t, J = 7.7 Hz, 4H), 2.53 (t, J = 7.9 Hz, 4H), 1.70−1.65 (m, 4H), 1.56−1.52 (m, 4H), 1.36−1.23 (m, 48H), 0.98−0.84 (m, 12H); ^{13}C{^{1}H} NMR (151 MHz, $CDCl_3$) δ 149.6, 145.3, 142.3, 140.5, 139.7, 137.2, 132.0, 130.8, 130.8, 129.2, 127.9, 127.3, 126.8, 125.7, 124.0, 97.3, 35.9, 35.4, 31.9, 31.7, 31.2, 31.1, 29.6, 29.6, 29.6, 29.4, 29.3, 29.3, 29.0, 22.7, 22.6, 14.1 (2 signals); HRMS (APCI): m/z calculated for $C_{72}H_{95}Cl_2N_4$: 1085.6934 [M + H]$^+$; found: 1085.6943.

3,3′-(1,4-Bis(4-dodecylphenyl)-1,4-dihydropyrrolo[3,2-b]-pyrrole-2,5-diyl)bis(2-chloro-7-(methylthio)quinoline) (4i). Off-white solid (394 mg, 39%); m.p.: 133−134 °C; ^{1}H NMR (600 MHz, $CDCl_3$) δ 7.96 (s, 2H), 7.68 (s, 2H), 7.54 (d, J = 8.6 Hz, 2H), 7.36 (d, J = 8.6 Hz, 2H), 7.16 (d, J = 7.9 Hz, 4H), 7.07 (d, J = 8.0 Hz, 4H), 6.58 (s, 2H), 2.59 (s, 6H), 2.54 (t, J = 7.9 Hz, 4H), 1.59−1.52 (m, 4H), 1.27−1.24 (m, 36H), 0.87 (t, J = 6.8 Hz, 6H) ^{13}C{^{1}H} NMR (126 MHz, $CDCl_3$) δ 151.0, 147.2, 143.1, 140.6, 139.8, 137.1, 130.8, 130.7, 129.2, 127.2, 126.4, 126.3, 124.2, 124.1, 121.6, 97.3,

https://doi.org/10.1021/acs.joc.3c02916
J. Org. Chem. 2024, 89, 4657−4672

35.4, 31.9, 31.2, 29.7, 29.6 (3 signals), 29.5, 29.3 (2 signals), 22.7, 14.9, 14.1; HRMS (APCI): m/z calculated for $C_{62}H_{75}Cl_2N_4S_2$: 1009.4810 $[M + H]^+$; found: 1009.4819.

3,3′-(1,4-Bis(3,5-di-tert-butylphenyl)-1,4-dihydropyrrolo-[3,2-b]pyrrole-2,5-diyl)bis(2-chloro-6-hexylquinoline) (4j). Pale yellow solid (400 mg, 41%); m.p.: 294−295 °C; ^{1}H NMR (500 MHz, $CDCl_3$) δ 8.04 (s, 2H), 7.88 (d, J = 8.6 Hz, 2H), 7.53 (d, J = 8.7 Hz, 2H), 7.45 (s, 2H), 7.17 (s, 2H), 7.09 (s, 4H), 6.58 (s, 2H), 2.76 (t, J = 7.6 Hz, 4H), 1.70−1.64 (m, 4H), 1.35−1.25 (m, 12H), 1.11 (s, 36H), 0.88 (t, J = 6.6 Hz, 6H); ^{13}C{^{1}H} NMR (151 MHz, THF-D_8) δ 151.5, 149.8, 145.7, 141.9, 139.8, 139.1, 131.6, 131.1, 130.3, 127.8 (2 signals), 126.9, 125.7, 118.8 (2 signals), 96.3, 35.6, 34.5, 31.7, 31.1, 30.6, 28.8, 22.5, 13.5; HRMS (APCI): m/z calculated for $C_{64}H_{79}Cl_2N_4$: 973.5682 $[M + H]^+$; found: 973.5690.

3,3′-(1,4-Bis(3,5-di-tert-butylphenyl)-1,4-dihydropyrrolo-[3,2-b]pyrrole-2,5-diyl)bis(2-chloro-6-methylquinoline) (4k). Pale yellow solid (392 mg, 47%); m.p.: 381−382 °C; ^{1}H NMR (500 MHz, $CDCl_3$) δ 8.05 (s, 2H), 7.88 (d, J = 8.6 Hz, 2H), 7.53 (dd, J = 8.6, 1.9 Hz, 2H), 7.17 (t, J = 1.8 Hz, 2H), 7.48 (s, 2H), 7.10 (d, J = 1.8 Hz, 4H), 6.58 (s, 2H), 2.52 (s, 6H), 1.12 (s, 36H); ^{13}C{^{1}H} NMR (126 MHz, $CDCl_3$) δ 151.8, 149.9, 145.2, 139.7, 138.7, 137.2, 132.7, 131.0, 130.3, 127.8, 127.6, 126.8, 126.2, 119.2, 119.1, 96.6, 34.8, 31.2, 21.6; HRMS (APCI): m/z calculated for $C_{54}H_{59}Cl_2N_4$: 833.4117 $[M + H]^+$; found: 833.4122.

3,3′-(1,4-Di(naphthalen-1-yl)-1,4-dihydropyrrolo[3,2-b]-pyrrole-2,5-diyl)bis(2-chloro-6-octylquinoline) (4l). Pale yellow solid (272 mg, 30%); m.p.: 208−209 °C; ^{1}H NMR (600 MHz, $CDCl_3$, mixture of atropisomers) δ 8.28 (d, J = 8.4 Hz, 1H), 8.11 (d, J = 8.4 Hz, 1H), 7.90 (d, J = 8.0 Hz, 1H), 7.87 (d, J = 8.0 Hz, 1H), 7.83 (s, 1H), 7.81 (s, 1H), 7.79−7.75 (m, 3H), 7.59 (t, J = 7.9 Hz, 1H), 7.57−7.47 (m, 3H), 7.45−7.40 (m, 2H), 7.38 (t, J = 7.8 Hz, 1H), 7.30 (t, J = 7.9 Hz, 1H), 7.25 (s, 3H), 7.21 (s, 1H), 7.19 (s, 1H), 6.38 (s, 1H), 6.36 (s, 1H), 2.64 (t, J = 7.9 Hz, 4H), 1.62−1.57 (m, 4H), 1.34−1.17 (m, 20H), 0.86 (t, J = 7.1 Hz, 6H); ^{13}C{^{1}H} NMR (126 MHz, $CDCl_3$, mixture of atropisomers) δ 149.3, 145.0, 142.0, 139.1, 135.8, 134.5, 132.9, 132.7, 131.8, 129.9, 129.7, 128.3, 128.2, 127.8, 127.6, 126.7, 126.5, 126.5, 125.6, 125.4, 124.2, 124.1, 98.4, 97.9, 35.8, 31.8, 31.1, 29.4, 29.2, 29.2, 22.6, 14.1; HRMS (APCI): m/z calculated for $C_{60}H_{59}Cl_2N_4$: 905.4117 $[M + H]^+$; found: 905.4118.

Typical Procedure for the Synthesis of 4,4′-(1,4-Bis(4-(*tert*-butyl)phenyl)-1,4-dihydropyrrolo[3,2-*b*]pyrrole-2,5-diyl)ditetrazolo[1,5-*a*]quinoline (6a). Glacial acetic acid (10 mL), toluene (10 mL), tetrazolo[1,5-*a*]quinoline-4-carbaldehyde (396 mg, 2 mmol, 2 equiv), and 4-(*tert*-butyl)aniline (299 mg, 2 mmol, 2 equiv) were placed in a 50 mL round-bottom flask equipped with a magnetic stir bar. The mixture reacted at 50 °C for 1 h. After that time, $Fe(ClO_4)_3 \cdot xH_2O$ (22 mg, 6 mol %) was added, followed by butane-2,3-dione (87 μL, 1 mmol, 1 equiv). The resulting mixture was stirred at 80 °C (oil bath) in an open flask under air for 2 h. Next, the heater was removed, and 5 mL of methanol was added to the reaction mixture, and the resulting mixture was stirred for 10 min. The precipitate was filtered, washed with methanol (5 mL) and diethyl ether (5 mL), recrystallized from dichloromethane/hexane mixture, and dried under vacuum affording 431 mg (61%) of pure product **6a** as a brown solid.

The procedure for the synthesis of compounds **6b−6r** is similar to that of compound **6a**.

4,4′-(1,4-Bis(4-(tert-butyl)phenyl)-1,4-dihydropyrrolo[3,2-b]pyrrole-2,5-diyl)ditetrazolo[1,5-a]quinoline (6a). Brown solid (431 mg, 61%); m.p.: 310−311 °C (dec.); ^{1}H NMR (600 MHz, $CDCl_3$) δ 8.61 (d, J = 7.8 Hz, 2H), 7.71 (td, J = 7.7, 1.1 Hz, 2H), 7.63 (s, 2H), 7.55 (td, J = 7.7, 1.1 Hz, 2H), 7.50 (d, J = 8.6 Hz, 4H), 7.44 (d, J = 7.9 Hz, 2H), 7.40 (d, J = 8.6 Hz, 4H), 7.18 (s, 2H), 1.40 (s, 18H); ^{13}C{^{1}H} NMR (126 MHz, tetrachloroethane-[D_2]) δ 150.5, 146.9, 136.6, 135.0, 130.0, 129.8, 128.6, 128.6, 128.3, 128.0, 126.9, 125.4, 124.2, 118.0, 116.5, 99.7, 34.7, 31.4; HRMS (APCI): m/z calculated for $C_{44}H_{39}N_{10}$: 707.3359 $[M + H]^+$; found: 707.3362.

4,4′-(1,4-Bis(4-(tert-butyl)phenyl)-1,4-dihydropyrrolo[3,2-b]pyrrole-2,5-diyl)bis(7-methyltetrazolo[1,5-a]quinoline) (6b). Brown solid (500 mg, 68%); m.p.: 318−319 °C (dec.); ^{1}H NMR (500 MHz, $CDCl_3$) δ 8.49 (d, J = 8.5 Hz, 2H), 7.61 (s, 2H), 7.53 (dd, J = 8.5, 1.7 Hz, 2H), 7.49 (d, J = 8.5 Hz, 4H), 7.39 (d, J = 8.5 Hz, 4H), 7.21 (s, 2H), 7.11 (s, 2H), 2.47 (s, 6H), 1.40 (s, 18H); ^{13}C{^{1}H} NMR (126 MHz, $CDCl_3$) δ 150.3, 146.8, 138.2, 137.1, 135.1, 131.2, 129.9, 127.9, 127.4, 126.9, 126.8, 125.6, 124.4, 118.2, 116.4, 100.0, 34.7, 31.4, 21.4; HRMS (APCI): m/z calculated for $C_{46}H_{43}N_{10}$: 735.3672 $[M + H]^+$; found: 735.3674.

4,4′-(1,4-Bis(3,4,5-trimethoxyphenyl)-1,4-dihydropyrrolo-[3,2-b]pyrrole-2,5-diyl)ditetrazolo[1,5-a]quinoline (6c). Cream solid (504 mg, 65%); m.p.: 322−323 °C (dec.); ^{1}H NMR (500 MHz, $CDCl_3$) δ 8.63 (d, J = 8.3 Hz, 2H), 7.75 (dt, J = 8.5, 4.2 Hz, 2H), 7.68 (s, 2H), 7.59 (d, J = 4.2 Hz, 4H), 7.33 (s, 2H), 6.72 (s, 4H), 3.97 (s, 6H), 3.77 (s, 12H); ^{13}C{^{1}H} NMR (126 MHz, tetrachloroethane-[D_2]) δ 153.6, 146.2, 136.8, 134.4, 134.2, 129.8, 129.2, 128.2, 128.0, 127.8, 127.1, 123.4, 117.1, 116.0, 103.2, 99.0, 60.6, 56.0; HRMS (APCI): m/z calculated for $C_{42}H_{35}N_{10}O_6$: 775.2741 $[M + H]^+$; found: 775.2742.

4,4′-(1,4-Bis(2,4-dimethoxyphenyl)-1,4-dihydropyrrolo-[3,2-b]pyrrole-2,5-diyl)ditetrazolo[1,5-a]quinoline (6d). Yellow solid (443 mg, 62%); m.p.: 316−317 °C (dec.); ^{1}H NMR (500 MHz, tetrachloroethane-[D_2], mixture of atropisomers) δ 7.92 (d, J = 8.3 Hz, 2H), 7.08 (dt, J = 8.4, 4.1 Hz, 2H), 6.89−6.94 (m, 4H), 6.72−6.79 (m, 3H), 6.64 (d, J = 6.7 Hz, 2H), 6.58 (d, J = 8.6 Hz, 1H), 6.06 (d, J = 2.6 Hz, 1H), 5.96−6.00 (m, 2H), 5.89 (dd, J = 8.5, 2.6 Hz, 1H), 3.25 (s, 3H), 3.23 (s, 3H), 3.14 (s, 3H), 2.96 (s, 3H); ^{13}C{^{1}H} NMR (126 MHz, tetrachloroethane-[D_2], mixture of atropisomers) δ 159.7, 154.8, 146.3, 134.8, 134.6, 130.5, 130.4, 129.2, 128.8, 128.6, 128.2, 127.9, 127.6, 125.6, 125.0, 123.8, 120.9, 120.8, 118.2, 118.0, 115.9, 104.7, 99.8, 99.7, 99.0, 98.3, 55.6, 55.4, 55.3; HRMS (APCI): m/z calculated for $C_{40}H_{31}N_{10}O_4$: 715.2530 $[M + H]^+$; found: 715.2524.

4,4′-(1,4-Bis(2-bromo-4-(tert-butyl)phenyl)-1,4-dihydropyrrolo[3,2-b]pyrrole-2,5-diyl)ditetrazolo[1,5-a]-quinoline (6e). Orange solid (363 mg, 42%); m.p.: 328−329 °C (dec.); ^{1}H NMR (500 MHz, tetrachloroethane-[D_2], mixture of atropisomers) δ 8.47 (d, J = 8.3 Hz, 2H), 7.72 (s, 1H), 7.68−7.61 (m, 3H), 7.53−7.42 (m, 6H), 7.40−7.30 (m, 4H), 6.97 (s, 2H), 1.31 (s, 18H); ^{13}C{^{1}H} NMR (126 MHz, tetrachloroethane-[D_2], mixture of atropisomers) δ 154.3, 154.2, 146.9, 136.3, 136.3, 135.2, 134.9, 131.5, 131.5, 131.4, 130.2, 129.8, 129.7, 128.8, 128.6, 126.7, 126.6, 126.3, 126.1, 124.6, 122.4, 122.2, 118.6, 118.4, 116.8, 100.6, 100.2, 35.2, 31.5; HRMS (APCI): m/z calculated for $C_{44}H_{37}Br_2N_{10}$: 863.1569 $[M + H]^+$; found: 863.1560.

4,4′-(1,4-Bis(2-bromo-4-(tert-butyl)phenyl)-1,4-dihydropyrrolo[3,2-b]pyrrole-2,5-diyl)bis(7-methyltetrazolo-

https://doi.org/10.1021/acs.joc.3c02916
J. Org. Chem. 2024, 89, 4657−4672

[1,5-a]quinoline) (6f). Orange solid (179 mg, 20%); m.p.: 338−339 °C; ^{1}H NMR (600 MHz, tetrachloroethane-[D_2], mixture of atropisomers) δ 8.38 (d, J = 1.3 Hz, 1H), 8.37 (d, J = 1.6 Hz, 1H), 7.74 (d, J = 2.1 Hz, 1H), 7.69 (d, J = 2.1 Hz, 1H), 7.53 (d, J = 8.2 Hz, 1H), 7.49 (d, J = 2.6 Hz, 2H), 7.48 (s, 1H), 7.47−7.45 (m, 2H), 7.40 (d, J = 2.0 Hz, 1H), 7.37 (d, J = 8.2 Hz, 1H), 7.12 (s, 1H), 7.10 (s, 1H), 6.93 (s, 1H), 6.92 (s, 1H), 2.40 (s, 6H), 1.34 (s, 9H), 1.34 (s, 9H); HRMS (APCI): m/z calculated for $C_{46}H_{41}Br_2N_{10}$: 891.1882 $[M + H]^+$; found: 891.1869.

Dimethyl 2,2′-(2,5-bis(7-methyltetrazolo[1,5-a]quinolin-4-yl)pyrrolo[3,2-b]pyrrole-1,4-diyl)dibenzoate (6g). Yellow solid (377 mg, 51%); m.p.: 249−250 °C (dec.); ^{1}H NMR (500 MHz, tetrachloroethane-[D_2], mixture of atropisomers) δ 7.81 (d, J = 4.2 Hz, 2H), 7.79 (d, J = 4.3 Hz, 2H), 7.29 (dt, J = 7.9, 1.7 Hz, 2H), 7.00 (dd, J = 3.2, 1.3 Hz, 2H), 6.95−6.88 (m, 4H), 6.73 (d, J = 1.1 Hz, 2H), 6.58 (d, J = 5.6 Hz, 2H), 6.40 (s, 1H), 6.39 (s, 1H), 2.90 (s, 3H), 2.87 (s, 3H), 1.82 (s, 6H); ^{13}C{^{1}H} NMR (126 MHz, tetrachloroethane-[D_2], mixture of atropisomers) δ 166.0, 165.8, 145.9, 145.9, 138.0, 138.0, 137.9, 134.5, 134.2, 133.0, 131.1, 131.0, 130.5, 128.9, 128.3, 128.3, 128.1, 127.7, 127.5, 127.1, 126.7, 126.2, 123.6, 123.6, 117.0, 116.9, 115.7, 98.8, 98.6, 52.1, 52.0, 20.8; HRMS (APCI): m/z calculated for $C_{42}H_{31}N_{10}O_4$: 739.2530 $[M + H]^+$; found: 739.2525.

4,4′-(1,4-Bis(4-dodecylphenyl)-1,4-dihydropyrrolo[3,2-b]-pyrrole-2,5-diyl)ditetrazolo[1,5-a]quinoline (6h). Off-white solid (559 mg, 60%); m.p.: 183−184 °C; ^{1}H NMR (500 MHz, $CDCl_3$) δ 8.55 (d, J = 8.2 Hz, 2H), 7.68 (t, J = 7.8 Hz, 2H), 7.58 (s, 2H), 7.51 (t, J = 7.5 Hz, 2H), 7.42 (d, J = 7.5 Hz, 2H), 7.37 (d, J = 7.8 Hz, 4H), 7.27 (d, J = 7.8 Hz, 4H), 7.14 (s, 2H), 2.69 (t, J = 7.6 Hz, 4H), 1.73−1.63 (m, 4H), 1.40−1.34 (m, 8H), 1.33−1.19 (m, 28H), 0.87 (t, J = 6.8 Hz, 6H); ^{13}C{^{1}H}NMR (126 MHz, $CDCl_3$) δ 146.8, 142.1, 137.2, 135.2, 129.8, 129.6, 128.6, 128.4, 127.9, 127.5, 125.9, 124.2, 118.1, 116.5, 100.0, 35.5, 31.9, 31.4, 29.7 (4 signals), 29.6, 29.4, 29.3, 22.7, 14.1; HRMS (APCI): m/z calculated for $C_{60}H_{71}N_{10}$: 931.5863 $[M + H]^+$; found: 931.5862.

4,4′-(1,4-Bis(4-dodecylphenyl)-1,4-dihydropyrrolo[3,2-b]-pyrrole-2,5-diyl)bis(7-methyltetrazolo[1,5-a]quinoline) (6i). Off-white solid (624 mg, 65%); m.p.: 238−239 °C; ^{1}H NMR (500 MHz, $CDCl_3$) δ 8.39 (d, J = 8.4 Hz, 2H), 7.55 (s, 2H), 7.48 (d, J = 8.4 Hz, 2H), 7.36 (d, J = 7.8 Hz, 4H), 7.26 (d, J = 8.1 Hz, 4H), 7.16 (s, 2H), 7.04 (s, 2H), 2.69 (t, J = 7.6 Hz, 4H), 2.46 (s, 6H), 1.73−1.63 (m, 4H), 1.41−1.34 (m, 8H), 1.32−1.21 (m, 28H), 0.87 (t, J = 6.8 Hz, 6H); ^{13}C{^{1}H} NMR (126 MHz, $CDCl_3$) δ 146.6, 141.9, 138.1, 137.3, 135.1, 131.1, 129.9, 129.8, 127.8, 127.4, 126.7, 125.8, 124.2, 118.0, 116.3, 99.9, 35.5, 31.9, 31.4, 29.7, 29.7, 29.7, 29.5, 29.4, 29.2, 22.7, 21.3, 14.1; HRMS (APCI): m/z calculated for $C_{62}H_{75}N_{10}$: 959.6176 $[M + H]^+$; found: 959.6185.

4,4′-(1,4-Bis(4-hexylphenyl)-1,4-dihydropyrrolo[3,2-b]-pyrrole-2,5-diyl)ditetrazolo[1,5-a]quinoline (6j). Yellow solid (473 mg, 62%); m.p.: 262−263 °C; ^{1}H NMR (600 MHz, $CDCl_3$) δ 8.60 (d, J = 8.8 Hz, 2H), 7.71 (ddd, J = 8.4, 7.2, 1.3 Hz, 2H), 7.59 (s, 2H), 7.52 (ddd, J = 8.4, 7.2, 1.3 Hz, 2H), 7.46 (d, J = 7.1 Hz, 2H), 7.37 (d, J = 8.3 Hz, 4H), 7.27 (d, J = 8.3 Hz, 4H), 7.18 (s, 2H), 2.68 (t, J = 7.6 Hz, 4H), 1.69−1.64 (m, 4H), 1.40−1.28 (m, 12H), 0.90 (t, J = 6.9 Hz, 6H); ^{13}C{^{1}H} NMR (151 MHz, $CDCl_3$) δ 146.8, 142.0, 137.2, 135.1, 129.8, 129.6, 128.6, 128.4, 127.9, 127.4, 125.9, 124.1, 118.1, 116.5, 100.0, 35.5, 31.7, 31.4, 28.9, 22.6, 14.1; HRMS (APCI): m/z calculated for $C_{48}H_{47}N_{10}$: 763.3985 $[M + H]^+$; found: 763.3988.

4,4′-(1,4-Bis(4-hexylphenyl)-1,4-dihydropyrrolo[3,2-b]-pyrrole-2,5-diyl)bis(7-methyltetrazolo[1,5-a]quinoline) (6k). Yellow solid (475 mg, 60%); m.p.: 256−257 °C; ^{1}H NMR (600 MHz, $CDCl_3$) δ 8.47 (d, J = 8.5 Hz, 2H), 7.57 (s, 2H), 7.51 (dd, J = 8.5, 1.8 Hz, 2H), 7.36 (d, J = 8.3 Hz, 4H), 7.26 (d, J = 8.3 Hz, 4H), 7.22 (s, 2H), 7.11 (s, 2H), 2.69 (t, J = 7.6 Hz, 4H), 2.46 (s, 6H), 1.68 (m, 4H), 1.40−1.26 (m, 12H), 0.89 (t, J = 6.9 Hz, 6H); ^{13}C{^{1}H} NMR (151 MHz, $CDCl_3$) δ 146.6, 141.9, 138.1, 137.3, 135.1, 131.1, 129.8, 129.8, 127.8, 127.4, 126.7, 125.8, 124.1, 118.0, 116.2, 99.9, 35.5, 31.7, 31.4, 28.9, 22.6, 21.3, 14.1; HRMS (APCI): m/z calculated for $C_{50}H_{51}N_{10}$: 791.4298 $[M + H]^+$; found: 791.4305.

4,4′-(1,4-Bis(3,5-di-tert-butylphenyl)-1,4-dihydropyrrolo-[3,2-b]pyrrole-2,5-diyl)ditetrazolo[1,5-a]quinoline (6l). Yellow solid (524 mg, 64%); m.p.: 323−324 °C (dec.); ^{1}H NMR (600 MHz, $CDCl_3$) δ 8.61 (d, J = 8.3 Hz, 2H), 7.53 (td, J = 8.4, 1.3 Hz, 2H), 7.66 (s, 2H), 7.53 (td, J = 8.4, 1.3 Hz, 2H), 7.47 (t, J = 1.8 Hz, 2H), 7.38 (d, J = 6.6 Hz, 2H), 7.32 (d, J = 1.8 Hz, 4H), 7.12 (s, 2H), 1.27 (s, 36H); ^{13}C{^{1}H} NMR (151 MHz, $CDCl_3$) δ 152.8, 147.0, 138.8, 134.8, 129.7, 129.6, 128.6, 128.3, 127.9, 127.3, 124.1, 120.9, 120.7, 118.3, 116.6, 99.5, 35.0, 31.4; HRMS (APCI): m/z calculated for $C_{52}H_{55}N_{10}$: 819.4611 $[M + H]^+$; found: 819.4608.

4,4′-(1,4-Bis(3,5-di-tert-butylphenyl)-1,4-dihydropyrrolo-[3,2-b]pyrrole-2,5-diyl)bis(7-methyltetrazolo[1,5-a]-quinoline) (6m). Yellow solid (443 mg, 61%); m.p.: 307−308 °C (dec.); ^{1}H NMR (600 MHz, $CDCl_3$, mixture of atropisomers) δ 8.49 (d, J = 8.4 Hz, 2H), 7.61 (s, 2H), 7.52 (d, J = 8.4 Hz, 2H), 7.45 (t, J = 1.9 Hz, 2H), 7.31 (s, 4H), 7.16 (s, 2H), 7.09 (s, 2H), 2.48 (s, 6H), 1.27 (s, 36H); ^{13}C{^{1}H} NMR (151 MHz, $CDCl_3$, mixture of atropisomers) δ 152.7, 146.9, 138.8, 138.0, 134.6, 131.2, 129.6, 127.7, 127.4, 126.8, 124.1, 120.8, 120.5, 118.2, 116.4, 99.5, 35.0, 31.3, 21.4; HRMS (APCI): m/z calculated for $C_{54}H_{59}N_{10}$: 847.4924 $[M + H]^+$; found: 847.4923.

4,4′-(1,4-Bis(2-bromo-4-(tert-butyl)phenyl)-1,4-dihydropyrrolo[3,2-b]pyrrole-2,5-diyl)bis(7-hexyltetrazolo-[1,5-a]quinoline) (6n). Yellow solid (496 mg, 48%); m.p.: 291−292 °C (dec.); ^{1}H NMR (500 MHz, $CDCl_3$) δ 8.49 (s, 1H), 8.47 (s, 1H), 7.86 (d, J = 2.1 Hz, 1H), 7.76 (d, J = 2.1 Hz, 1H), 7.62 (d, J = 2.8 Hz, 2H), 7.57 (d, J = 8.2 Hz, 1H), 7.52 (s, 1H), 7.51 (s, 1H), 7.39 (dd, J = 8.3, 2.1 Hz, 1H), 7.28 (s, 1H), 7.17 (s, 1H), 7.13 (s, 1H), 6.98 (s, 1H), 6.97 (s, 2H), 2.71 (t, J = 6.9 Hz, 4H), 1.67−1.59 (m, 4H), 1.42 (s, 9H), 1.41 (s, 9H), 1.34−1.26 (m, 12H), 0.88 (t, J = 6.4 Hz, 6H); ^{13}C{^{1}H} NMR (126 MHz, $CDCl_3$) δ 153.7, 153.6, 146.6, 146.6, 143.2, 143.2, 136.5, 136.4, 135.0, 134.6, 131.2, 131.2, 131.1, 130.6, 130.6, 129.8, 129.7, 127.3, 127.2, 127.1, 127.0, 126.2, 126.1, 126.0, 125.6, 124.5, 122.2, 122.1, 118.4, 118.1, 116.4, 116.4, 100.8, 100.0, 35.7, 35.0, 35.0, 31.6, 31.2, 28.8, 28.8, 22.5, 14.0; HRMS (APCI): m/z calculated for $C_{56}H_{61}Br_2N_{10}$: 1031.3442 $[M + H]^+$; found: 1031.3451.

4,4′-(1,4-Bis(2-bromo-4-dodecylphenyl)-1,4-dihydropyrrolo[3,2-b]pyrrole-2,5-diyl)bis(7-methyltetrazolo-[1,5-a]quinoline) (6o). Yellow solid (581 mg, 52%); m.p.: 271−272 °C; ^{1}H NMR (500 MHz, $CDCl_3$) δ 8.49 (d, J = 8.3 Hz, 2H), 7.69 (s, 1H), 7.60 (s, 3H), 7.56 (d, J = 7.6 Hz, 1H), 7.54 (s, 1H), 7.52 (s, 1H), 7.32 (d, J = 7.9 Hz, 1H), 7.24 (s, 2H), 7.23−7.16 (m, 2H), 7.03 (s, 2H), 2.74 (t, J = 7.4 Hz, 2H), 2.72 (t, J = 7.4 Hz, 2H), 2.49 (s, 6H), 1.77−1.66 (m, 4H), 1.46−1.36 (m, 8H), 1.35−1.21 (m, 28H), 0.90 (t, J = 6.7

https://doi.org/10.1021/acs.joc.3c02916
J. Org. Chem. 2024, 89, 4657−4672

Hz, 6H); $^{13}C\{^{1}H\}$ NMR (126 MHz, $CDCl_3$) δ 145.3, 138.1, 136.6, 135.1, 134.7, 133.9, 131.2, 130.0, 129.0, 128.0, 126.1, 125.4, 124.5, 118.3, 116.4, 100.8, 100.0, 35.3, 31.9, 31.2, 29.7, 29.7, 29.7, 29.6, 29.5, 29.4, 29.2, 22.7, 21.3, 14.1; HRMS (APCI): m/z calculated for $C_{62}H_{73}Br_2N_{10}$: 1115.4386 $[M + H]^+$; found: 1115.4421.

4,4′-(1,4-Bis(2-bromo-4-dodecylphenyl)-1,4-dihydropyrrolo[3,2-b]pyrrole-2,5-diyl)bis(7-octyltetrazolo-[1,5-a]quinoline) (6p). Pale yellow solid (618 mg, 47%); m.p.: 245−246 °C (dec.); ^{1}H NMR (500 MHz, $CDCl_3$, mixture of atropisomers) δ 8.57−8.46 (m, 2H), 7.70−7.52 (m, 6H), 7.34−7.18 (m, 6H), 7.08−7.02 (m, 2H), 2.83−2.65 (m, 8H), 1.77−1.63 (m, 8H), 1.46−1.16 (m, 56H), 0.95−0.81 (m, 12H); $^{13}C\{^{1}H\}$ NMR (126 MHz, $CDCl_3$, mixture of atropisomers) δ 146.6 (2 signals), 145.4, 145.3, 143.2, 143.1, 139.1, 136.6, 135.1, 134.6, 133.9 (2 signals), 131.3, 131.2, 130.5 (2 signals), 130.0, 129.9, 129.1, 128.9, 127.4, 127.3, 127.0, 126.3, 125.6, 124.5, 124.4, 122.1, 122.0, 118.4, 118.2, 116.5, 116.4, 100.8, 100.0, 35.7, 35.3, 31.9, 31.8, 31.4, 31.3 (2 signals), 29.7 (3 signals), 29.6 (2 signals), 29.4 (2 signals), 29.3, 29.2, 22.7, 22.6, 14.1 (2 signals); HRMS (APCI): m/z calculated for $C_{76}H_{101}Br_2N_{10}$: 1311.6577 $[M + H]^+$; found: 1311.6583.

4,4′-(1,4-Bis(2-bromonaphthalen-1-yl)-1,4-dihydropyrrolo[3,2-b]pyrrole-2,5-diyl)bis(7-hexyltetrazolo-[1,5-a]quinoline) (6q). Pale yellow solid (439 mg, 43%); m.p.: 227−228 °C (dec.); ^{1}H NMR (500 MHz, $CDCl_3$, mixture of atropisomers) δ 8.38 (dd, J = 8.5, 2.8 Hz, 2H), 7.98 (d, J = 8.8 Hz, 2H), 7.95 (d, J = 8.8 Hz, 2H), 7.90 (d, J = 8.8 Hz, 1H), 7.87 (d, J = 8.8 Hz, 1H), 7.64 (d, J = 8.4 Hz, 1H), 7.61 (d, J = 4.7 Hz, 2H), 7.59−7.51 (m, 3H), 7.48 (d, J = 7.7 Hz, 2H), 7.44 (d, J = 8.2 Hz, 2H), 6.96 (s, 1H), 7.00 (s, 1H), 6.93 (s, 1H), 6.90 (s, 1H), 2.66−2.58 (m, 4H), 1.62−1.51 (m, 4H), 1.33−1.22 (m, 12H), 0.83−0.87 (m, 6H); $^{13}C\{^{1}H\}$ NMR (126 MHz, $CDCl_3$, mixture of atropisomers) δ 146.3, 143.1, 135.3, 135.0, 134.9, 133.4 (2 signals), 132.8, 132.7, 132.5, 132.4, 130.5 (2 signals), 130.1, 128.8 (2 signals), 128.3, 127.3 (2 signals), 127.0, 124.8, 124.7, 124.3, 123.3, 123.1, 122.4, 122.3, 118.1, 116.3, 100.2, 100.1, 35.6, 31.6, 31.3, 28.8, 22.6, 14.1; HRMS (APCI): m/z calculated for $C_{56}H_{49}Br_2N_{10}$: 1019.2508 $[M + H]^+$; found: 1019.2520.

4,4′-(1,4-Bis(10-bromophenanthren-9-yl)-1,4-dihydropyrrolo[3,2-b]pyrrole-2,5-diyl)bis(7-octyltetrazolo-[1,5-a]quinoline) (6r). Brown solid (424 mg, 36%); m.p.: 231−232 °C (dec.); ^{1}H NMR (500 MHz, $CDCl_3$) δ 9.23 (s, 2H), 8.91 (s, 2H), 8.63 (d, J = 8.2 Hz, 4H), 8.50 (d, J = 8.6 Hz, 2H), 8.39 (d, J = 8.0 Hz, 2H), 7.87 (d, J = 8.2 Hz, 2H), 7.83 (s, 2H), 7.89−7.63 (m, 8H), 7.49 (t, J = 7.5 Hz, 2H), 2.75 (t, J = 7.7 Hz, 4H), 1.74−1.62 (m, 4H), 1.40−1.22 (m, 20H), 0.88 (t, J = 6.7 Hz, 6H); $^{13}C\{^{1}H\}$ NMR (126 MHz, $CDCl_3$) δ 160.2, 146.7, 146.3, 143.7, 133.5, 132.0, 130.6, 129.8, 129.6, 129.3 (2 signals), 128.4, 127.9, 127.5, 127.2, 127.1, 126.4, 124.6, 123.6, 122.8, 122.6, 120.5, 116.6, 108.6, 35.6, 31.8, 31.1, 29.4, 29.2 (2 signals), 22.7, 14.1; HRMS (APCI): m/z calculated for $C_{68}H_{61}Br_2N_{10}$: 1175.3442 $[M + H]^+$; found: 1175.3443.

Typical Procedure for the Synthesis of 7,19-Didodecyl-2,14-dihexyldibenzo[*b*,*h*]benzo[5′,6′]quino-[2″,3″:7′,8′]indolizino[3′,2′:4,5]pyrrolo[2,1-*f*]-1,6-naphthyridine (10a). A Schenk flask was charged with chloroquinoline-containing pyrrolopyrrole **4h** (44.0 mg, 0.04 mmol, 1 equiv), Ph_3P (10.5 mg, 0.04 mmol, 1 equiv), Cs_2CO_3 (58.5 mg, 0.18 mmol, 4.5 equiv), and $Pd(OAc)_2$ (3.6 mg, 40 mol %). Then, dry *m*-xylene (3 mL) was added, and the resulting mixture was degassed 3 times (by evacuation and refilling with argon) and stirred at 160 °C overnight. After cooling to around 80 °C, toluene (10 mL) was added, and the resulting suspension was passed through a pad of Celite. Next, the product was washed from the Celite pad with boiling toluene, all filtrates were concentrated to *ca.* 2 mL and 36.5 mg (90%) of **10a** as orange solid was filtered off. The dried product **10a** obtained was pure enough for all analytical purposes.

The procedure for the synthesis of compounds **10b** and **10c** is similar to that of compound **10a**.

7,19-Didodecyl-2,14-dihexyldibenzo[b,h]benzo[5′,6′]-quino[2″,3″:7′,8′]indolizino[3′,2′:4,5]pyrrolo[2,1-f]-1,6-naphthyridine (10a). Orange solid (36.5 mg, 90%); m.p.: 305−306 °C (dec.); ^{1}H NMR (500 MHz, Benzene-d_6) δ 9.35 (d, J = 7.2 Hz, 2H), 8.30 (dd, J = 8.5, 3.9 Hz, 2H), 8.05 (d, J = 8.4 Hz, 2H), 7.81−7.78 (m, 2H), 7.47−7.43 (m, 4H), 7.31−7.29 (m, 2H), 6.97 (s, 1H), 6.96 (d, J = 11.0 Hz, 1H), 2.79 (t, J = 7.9 Hz, 4H), 2.71 (t, J = 7.8 Hz, 4H), 1.84−1.79 (m, 4H), 1.74−1.71 (m, 4H), 1.53−1.24 (m, 48H), 0.97 (t, J = 6.8 Hz, 6H), 0.91 (t, J = 6.8 Hz, 6H); $^{13}C\{^{1}H\}$ NMR (126 MHz, tetrachloroethane-[D_2]) δ 145.7, 143.9, 141.0, 137.7, 134.6, 130.6, 130.3, 129.2, 127.8, 126.8, 126.4, 125.7, 125.1, 122.2, 120.4, 114.8, 99.7, 89.3, 36.0, 35.7, 31.9, 31.8, 31.4, 30.8, 29.7, 29.6 (2 signals), 29.3, 29.1, 22.6, 14.0, 13.9; HRMS (APCI): m/z calculated for $C_{72}H_{93}N_4$: 1013.7400 $[M + H]^+$; found: 1013.7426.

7,19-Didodecyl-3,15-bis(methylthio)dibenzo[b,h]benzo-[5′,6′]quino[2″,3″:7′,8′]indolizino[3′,2′:4,5]pyrrolo[2,1-f]-1,6-naphthyridine (10b). Red solid (14.7 mg, 39%); m.p.: 323−324 °C (dec.); ^{1}H NMR (500 MHz, tetrachloroethane-[D_2]) δ 8.76 (s, 2H), 8.06−8.20 (br. s, 2H), 7.71−7.69 (m, 4H), 7.55−7.48 (br. s, 2H), 7.44 (d, J = 8.2 Hz, 2H), 7.29 (d, J = 8.2 Hz, 2H), 6.85−6.99 (br. s, 2H), 2.83 (t, J = 7.9 Hz, 4H), 2.64 (s, 6H), 1.82−1.85 (m, 4H), 1.50−1.55 (m, 4H), 1.43−1.49 (m, 4H), 1.26−1.40 (m, 28H), 0.87 (t, J = 6.8 Hz, 6H); HRMS (APCI): m/z calculated for $C_{62}H_{73}N_4S_2$: 937.5277 $[M + H]^+$; found: 937.5278.

2,16-Dioctylbenzo[b]naphtho[1,2-h]naphtho[1″,2″:5′,6′]-quino[2″,3″:7′,8′]indolizino[3′,2′:4,5]pyrrolo[2,1-f]-1,6-naphthyridine (10c). Orange solid (11.7 mg, 35%); m.p.: 295−296 °C (dec.); ^{1}H NMR (500 MHz, $CDCl_3$) δ 9.25 (d, J = 7.1 Hz, 2H), 9.20 (d, J = 8.6 Hz, 2H), 8.52 (s, 2H), 8.07 (d, J = 8.6 Hz, 2H), 8.05 (dd, J = 8.6, 2.4 Hz, 2H), 7.90 (d, J = 8.6 Hz, 2H), 7.75−7.72 (m, 4H), 7.62 (s, 2H), 7.52 (dd, J = 8.6, 1.9 Hz, 2H), 7.21 (s, 2H), 2.80 (t, J = 7.8 Hz, 4H), 1.76−1.73 (m, 4H), 1.44−1.24 (m, 20H), 0.88 (t, J = 6.7 Hz, 6H); $^{13}C\{^{1}H\}$ NMR (126 MHz, $CDCl_3$) δ 146.2, 144.4, 141.3, 135.6, 133.1, 131.9, 131.8, 130.8, 129.3, 128.5, 127.8, 127.4, 126.2, 125.4, 124.8, 124.6, 124.5, 123.4, 122.8, 121.1, 120.8, 95.5, 36.0, 31.9, 31.1, 29.5, 29.4, 29.3, 22.7, 14.1; HRMS (APCI): m/z calculated for $C_{60}H_{57}N_4$: 833.4583 $[M + H]^+$; found: 833.4585.

Typical Procedure for the Synthesis of 10,24-Didodecyl-7,21-dimethyldibenzo[*c*,*f*]benzo[5′,6′]-tetrazolo[1‴,5‴:1″,2″]quino[4″,3″:7′,8′]indolizino-[3′,2′:4,5]pyrrolo[2,1-*a*]tetrazolo[1,5-*h*]-2,7-naphthyridine (11a). A Schenk flask was charged with dibrominated tetrazoloquinoline-containing pyrrolopyrrole **6o** (90.0 mg, 0.08 mmol, 1 equiv), Ph_3P (21.0 mg, 0.08 mmol, 1 equiv), Cs_2CO_3 (117.0 mg, 0.36 mmol, 4.5 equiv), and $Pd(OAc)_2$ (7.2 mg, 40

https://doi.org/10.1021/acs.joc.3c02916
J. Org. Chem. 2024, 89, 4657−4672

mixture degassed 3 times (by evacuation and refilling with Argon) and stirred at 160 °C for 20 h. After cooling to around 80 °C, toluene (10 mL) was added and resulting suspension was passed through a pad of Celite. Next, the product was washed from the Celite pad with boiling toluene, and all filtrates were concentrated to *ca.* 1 mL. Next, 1 mL of chloroform was added, and the flask with reaction mixture was moved to the fridge. Upon 8 h, 35.0 mg (45%) of compound **11a** was filtered as dark purple fine crystals. The dried product **11a** obtained was pure enough for all analytical purposes.

The procedure for the synthesis of compounds **11b**−**11d** is similar to that of compound **11a**, except that compounds **11c** and **11d** were purified by column chromatography (SiO_2, EtOAc:hexanes, 20:80, than 25:75).

10,24-Didodecyl-7,21-dimethyldibenzo[c,f]benzo[5′,6′]-tetrazolo[1‴,5‴:1″,2″]quino[4″,3″:7′,8′]indolizino[3′,2′:4,5]-pyrrolo[2,1-a]tetrazolo[1,5-h]-2,7-naphthyridine (11a). Dark purple solid (35.0 mg, 45%); m.p.: 296−297 °C (dec.); ^{1}H NMR (600 MHz, $CDCl_3$) δ 8.40 (s, 2H), 8.33 (d, J = 8.1 Hz, 2H), 8.08 (s, 2H), 7.89 (s, 2H), 7.76 (d, J = 8.1 Hz, 2H), 7.43 (d, J = 8.2 Hz, 2H), 7.23 (d, J = 8.2 Hz, 2H), 2.68 (t, J = 7.9 Hz, 4H), 2.58 (s, 6H), 1.75−1.70 (m, 4H), 1.44−1.40 (m, 4H), 1.39−1.24 (m, 32H), 0.88 (t, J = 6.9 Hz, 6H); ^{13}C{^{1}H} NMR (126 MHz, $CDCl_3$) δ 144.5, 137.5, 137.1, 133.2, 130.7, 129.9, 128.4, 127.7, 127.2, 127.0, 124.0, 122.6, 121.8, 117.0, 115.7, 111.7, 92.7, 35.6, 31.9, 31.4, 31.4, 30.2, 29.8, 29.7, 29.7, 29.4, 29.4, 22.7, 21.9, 14.1; HRMS (APCI): m/z calculated for $C_{62}H_{71}N_{10}$: 955.5863 $[M + H]^+$; found: 955.5852.

10,24-Didodecyl-7,21-dioctyldibenzo[c,f]benzo[5′,6′]-tetrazolo[1‴,5‴:1″,2″]quino[4″,3″:7′,8′]indolizino[3′,2′:4,5]-pyrrolo[2,1-a]tetrazolo[1,5-h]-2,7-naphthyridine (11b). Dark purple solid (43.3 mg, 47%); m.p.: 312−313 °C (dec.); ^{1}H NMR (500 MHz, $CDCl_3$) δ 8.42 (s, 2H), 8.37 (d, J = 8.2 Hz, 2H), 8.11 (s, 2H), 7.98 (s, 2H), 7.87 (d, J = 8.2 Hz, 2H), 7.45 (dd, J = 8.3, 1.5 Hz, 2H), 7.31 (d, J = 8.2 Hz, 2H), 2.80 (t, J = 7.9 Hz, 4H), 2.71 (t, J = 7.9 Hz, 4H), 1.83−1.78 (m, 4H), 1.76−1.70 (m, 4H), 1.52−1.25 (m, 56H), 0.91 (t, J = 7.2 Hz, 6H), 0.86 (t, J = 7.2 Hz, 6H); ^{13}C{^{1}H} NMR (126 MHz, $CDCl_3$) δ 144.3, 142.3, 136.9, 133.0, 130.6, 129.1, 128.0, 127.8, 127.5, 127.2, 126.8, 122.4, 121.6, 118.0, 116.8, 115.5, 111.4, 92.6, 36.2, 35.7, 32.0, 31.9, 31.7, 31.5, 29.8, 29.8, 29.8, 29.7, 29.7, 29.6, 29.5, 29.4, 29.4, 22.7, 22.7, 14.1, 14.2; HRMS (APCI): m/z calculated for $C_{76}H_{98}N_{10}$: 1150.7976 $[M]^+$; found: 1150.7977.

7,23-Dihexylbenzo[c]naphtho[2,1-f]naphtho[1″,2″:5′,6′]-tetrazolo[1‴,5‴:1″,2″]quino[4″,3″:7′,8′]indolizino[3′,2′:4,5]-pyrrolo[1,2-h]tetrazolo[5,1-a]-2,7-naphthyridine (11c). Purple solid (26.8 mg, 39%); m.p.: 301−302 °C (dec.); ^{1}H NMR (500 MHz, $CDCl_3$) δ 8.97 (d, J = 8.7 Hz, 2H), 8.95 (s, 2H), 8.58 (d, J = 8.4 Hz, 2H), 8.40 (d, J = 8.9 Hz, 2H), 7.71 (dd, J = 8.2, 1.6 Hz, 2H), 7.63 (d, J = 8.0 Hz, 2H), 7.59 (d, J = 8.8 Hz, 2H), 7.44−7.39 (br. s, 2H), 7.35 (t, J = 7.7 Hz, 2H), 7.29 (t, J = 7.7 Hz, 2H), 3.14 (t, J = 7.8 Hz, 4H), 2.09−2.04 (m, 4H), 1.70−1.64 (m, 4H), 1.58−1.55 (m, 2H), 1.53−1.51 (m, 2H), 1.49−1.42 (m, 4H), 0.98 (t, J = 7.2 Hz, 6H); ^{13}C{^{1}H} NMR (151 MHz, CD_2Cl_2) δ 149.1, 144.6, 142.9, 133.1, 132.1, 130.1, 128.9, 128.6, 128.5, 127.9, 127.7, 124.8, 124.4, 124.0, 123.8, 123.5, 122.7, 120.3, 117.6, 113.4, 111.7, 95.5, 36.6, 32.2, 31.9, 29.6, 23.2, 14.3; HRMS (APCI): m/z calculated for $C_{56}H_{47}N_{10}$: 859.3985 $[M + H]^+$; found: 859.3992.

7-Octyl-19-(7-octyltetrazolo[1,5-a]quinolin-4-yl)-20-(9-phenanthryl)-20H-benzo[c]phenanthro[9,10-f]pyrrolo-[2′,3′:4,5]pyrrolo[1,2-h]tetrazolo[5,1-a]-2,7-naphthyridine (11d). Purple solid (21.2 mg, 26%); m.p.: 286−287 °C (dec.); ^{1}H NMR (600 MHz, $CDCl_3$) δ 9.40−9.38 (m, 1H); 8.87−7.29 (complex multiplets, 24H), 6.83 (d, J = 8.4 Hz, 1H), 2.53−2.48 (m, 4H), 1.50−1.43 (m, 4H), 1.31−1.17 (m, 20H), 0.88−0.83 (m, 6H); ^{13}C{^{1}H}NMR (126 MHz, CD_2Cl_2) δ 145.3, 143.2, 141.6, 140.0, 139.8, 135.6, 134.6, 131.9, 131.6, 131.3, 130.8, 130.5, 130.4, 130.4, 130.2, 129.8, 129.5, 129.4, 129.1, 129.0, 127.9, 127.8, 127.7, 127.6, 127.5, 127.4, 127.4, 127.3, 127.2, 127.1, 126.8, 126.7, 126.3, 126.2, 126.2, 125.6, 124.7, 124.5, 124.0, 124.0, 123.8, 123.5, 123.3, 122.9, 122.1, 117.9, 116.7, 116.0, 112.5, 105.3, 105.0, 91.4, 91.2, 35.8, 35.4, 31.8, 31.8, 31.2, 29.7, 29.3, 29.3, 29.1, 29.1, 29.1, 22.6, 22.6, 13.9, 13.8; HRMS (APCI): m/z calculated for $C_{68}H_{61}N_{10}$: 1017.5081 $[M + H]^+$; found: 1017.5085.

■ ASSOCIATED CONTENT

Data Availability Statement

The data underlying this study are available in the published article and its Supporting Information.

Supporting Information

The Supporting Information is available free of charge at https://pubs.acs.org/doi/10.1021/acs.joc.3c02916.

Theoretical data; typical procedure for the synthesis of **4a**, **6a**, **10a**, **11a**; spectral data, ^{1}H and ^{13}C NMR spectra, optical properties, and photophysical data of **4a**−**4l**, **6a**−**6r**, **10a**−**10c**, **11a**−**11d**; crystallographic data of **4k**, **6j**, **10a**, **11d** (PDF)

Accession Codes

CCDC 2297032, 2297034−2297035, and 2297398 contain the supplementary crystallographic data for this paper. These data can be obtained free of charge via www.ccdc.cam.ac.uk/data_request/cif, or by emailing data_request@ccdc.cam.ac.uk, or by contacting The Cambridge Crystallographic Data Centre, 12 Union Road, Cambridge CB2 1EZ, UK; fax: +44 1223 336 033.

■ AUTHOR INFORMATION

Corresponding Authors

Mohammad B. Teimouri − *Institute of Organic Chemistry, Polish Academy of Sciences, Warsaw 01-224, Poland; Faculty of Chemistry, Kharazmi University, Tehran 15719-14911, Iran;* orcid.org/0000-0003-4178-9995; Email: teimouri@khu.ac.ir

Michał K. Cyrański − *Faculty of Chemistry, University of Warsaw, Warsaw 02-093, Poland*; Email: mkc@chem.uw.edu.pl

Aleksander Rebane − *National Institute for Chemical Physics and Biophysics, Tallinn 12618, Estonia; Department of Physics, Montana State University, Bozeman, Montana 59717, United States;* orcid.org/0000-0003-4330-5544; Email: arebane@montana.edu

Daniel T. Gryko − *Institute of Organic Chemistry, Polish Academy of Sciences, Warsaw 01-224, Poland;* orcid.org/0000-0002-2146-1282; Email: dtgryko@icho.edu

Authors

Irena Deperasińska − *Institute of Physics of Polish Academy of Sciences, Polish Academy of Sciences, Warsaw 02-668, Poland*

Matt Rammo − *National Institute for Chemical Physics and Biophysics, Tallinn 12618, Estonia*

Marzena Banasiewicz − *Institute of Physics of Polish Academy of Sciences, Polish Academy of Sciences, Warsaw 02-668, Poland;* orcid.org/0000-0002-8251-5440

Charles W. Stark − *National Institute for Chemical Physics and Biophysics, Tallinn 12618, Estonia;* orcid.org/0000-0002-8998-8638

Łukasz Dobrzycki − *Faculty of Chemistry, University of Warsaw, Warsaw 02-093, Poland;* orcid.org/0000-0002-4426-963X

Complete contact information is available at: https://pubs.acs.org/10.1021/acs.joc.3c02916

Author Contributions

The manuscript was written through contributions of all authors. All authors have given approval to the final version of the manuscript.

Notes

The authors declare no competing financial interest.

■ ACKNOWLEDGMENTS

This work was supported by the Polish National Science Center, Poland (grants OPUS 2020/37/B/ST4/00017 and HARMONIA 2018/30/M/ST5/00460), the Foundation for Polish Science (TEAM POIR.04.04.00-00-3CF4/16-00). This project has received funding from the European Union's Horizon 2020 research and innovation programme under the Marie Skłodowka-Curie grant agreement No 101007804. Calculations were performed at the Interdisciplinary Center for Mathematical and Computational Modeling (ICM) University of Warsaw under computational allocation G95-1734. M.B.T. thanks Kharazmi University Research Council for the financial support of his sabbatical leave. The authors also thank Dr David C. Young for proofreading the manuscript.

■ REFERENCES

(1) (a) Messersmith, R. E.; Siegler, M. A.; Tovar, J. D. Aromaticity Competition in Differentially Fused Borepin-Containing Polycyclic Aromatics. *J. Org. Chem.* **2016**, *81*, 5595−5605. (b) Tamba, S.; Nitani, N.; Seo, T.; Nitta, H.; Tanaka, K.; Hagiya, H.; Aso, Y.; Ie, Y. Tetrazolo[1,5-*a*]pyridine-Containing π-Conjugated Systems: Synthesis, Properties, and Semiconducting Characteristics. *Org. Lett.* **2022**, *24*, 3792−3796. (c) Borissov, A.; Maurya, Y. K.; Moshniaha, L.; Wong, W.-S.; Żyła-Karwowska, M.; Stępień, M. Recent Advances in Heterocyclic Nanographenes and Other Polycyclic Heteroaromatic Compounds. *Chem. Rev.* **2022**, *122*, 565−788. (d) Oki, K.; Takase, M.; Mori, S.; Shiotari, A.; Sugimoto, Y.; Ohara, K.; Okujima, T.; Uno, H. Synthesis, Structures, and Properties of Core-Expanded Azacorronene Analogue: A Twisted π-System with Two N-Doped Heptagons. *J. Am. Chem. Soc.* **2018**, *140*, 10430−10434. (e) Wagner, J.; Crocomo, P. Z.; Kochman, M. A.; Kubas, A.; Data, P.; Lindner, M. Modular Nitrogen-Doped Concave Polycyclic Aromatic Hydrocarbons for High-Performance Organic Light-Emitting Diodes with Tunable Emission Mechanisms. *Angew. Chem., Int. Ed.* **2022**, *61*, No. e202202232. (f) Qiu, Z.-L.; Chen, X.-W.; Huang, Y.-D.; Wei, R.-J.; Chu, K.-S.; Zhao, X.-J.; Tan, Y.-Z. Nanographene with Multiple Embedded Heptagons: Cascade Radical Photocyclization. *Angew. Chem., Int. Ed.* **2022**, *61*, No. e202116955. (g) Barker, J. E.; Dressler, J. J.; Valdivia, A. C.; Kishi, R.; Strand, E. T.; Zakharov, L. N.; MacMillan, S. N.; Gómez-García, C. J.; Nakano, M.; Casado, J.; Haley, M. M. Molecule Isomerism Modulates the Diradical Properties of Stable Singlet Diradicaloids. *J. Am. Chem. Soc.* **2020**, *142*, 1548−1555.

(2) (a) Terenti, N.; Giurgi, G.-I.; Crişan, A. P.; Anghel, C.; Bogdan, A.; Pop, A.; Stroia, I.; Terec, A.; Szolga, L.; Grosu, I.; Roncali, J. Structure−properties of small donor−acceptor molecules for homojunction single-material organic solar cells. *J. Mater. Chem. C* **2022**, *10*, 5716−5726. (b) Wang, Y.; Michinobu, T. Benzothiadiazole and its π-extended, heteroannulated derivatives: useful acceptor building blocks for high-performance donor−acceptor polymers in organic electronics. *J. Mater. Chem. C* **2016**, *4*, 6200−6214. (c) Wang, Y.-F.; Lu, H.-Y.; Chen, C.; Li, M.; Chen, C.-F. 1,8-Naphthalimide-based circularly polarized TADF enantiomers as the emitters for efficient orange-red OLEDs. *Organic Mater.* **2019**, *70*, 71−77. (d) Eftaiha, A. F.; Sun, J.-P.; Hill, I. G.; Welch, G. C. Recent advances of non-fullerene, small molecular acceptors for solution processed bulk heterojunction solar cells. *J. Mater. Chem. A* **2014**, *2*, 1201−1213.

(3) Stecko, S.; Gryko, D. T. Multifunctional Heteropentalenes: From Synthesis to Optoelectronic Applications. *JACS Au* **2022**, *2*, 1290−1305.

(4) Sanil, G.; Koszarna, B.; Poronik, Y. M.; Vakuliuk, O.; Szymański, B.; Kusy, D.; Gryko, D. T. The chemistry of 1,4-dihydropyrrolo[3,2-*b*]pyrroles. *Adv. Heterocycl. Chem.* **2022**, *138*, 335−409.

(5) Liu, H.; Ye, J.; Zhou, Y.; Fu, L.; Lu, Q.; Zhang, C. New pyrrolo[3,2-*b*]pyrrole derivatives with multiple-acceptor substitution: Efficient fluorescent emission and near-infrared two-photon absorption. *Tetrahedron Lett.* **2017**, *58*, 4841−4844.

(6) Ivanov, A. I.; Dereka, B.; Vauthey, E. A simple model of solvent-induced symmetry-breaking charge transfer in excited quadrupolar molecules. *J. Chem. Phys.* **2017**, *146*, 164306.

(7) Friese, D. H.; Mikhaylov, A.; Krzeszewski, M.; Poronik, Y. M.; Rebane, A.; Ruud, K.; Gryko, D. T. Pyrrolo[3,2- b]pyrroles—From Unprecedented Solvatofluorochromism to Two-Photon Absorption. *Chem.-Eur. J.* **2015**, *21*, 18364−18374.

(8) Wu, D.; Zheng, J.; Xu, C.; Kang, D.; Hong, W.; Duan, Z.; Mathey, F. Phosphindole fused pyrrolo[3,2-*b*]pyrroles: a new single-molecule junction for charge transport. *Dalton Trans.* **2019**, *48*, 6347−6352.

(9) Antonyová, V.; Tatar, A.; Brogyányi, T.; Kejík, Z.; Kaplánek, R.; Vellieux, F.; Abramenko, N.; Sinica, A.; Hajduch, J.; Novotný, P.; et al.et al. Targeting of the Mitochondrial TET1 Protein by Pyrrolo[3,2-*b*]pyrrole Chelators. *Int. J. Mol. Sci.* **2022**, *23*, 10850−10875.

(10) Dereka, B.; Vauthey, E. Direct local solvent probing by transient infrared spectroscopy reveals the mechanism of hydrogen-bond induced nonradiative deactivation. *Chem. Sci.* **2017**, *8*, 5057−5066.

(11) Wu, J.-Y.; Yu, C.-H.; Wen, J.-J.; Chang, C.-L.; Leung, M. Pyrrolo[3,2-*b*]pyrroles for Photochromic Analysis of Halocarbons. *Anal. Chem.* **2016**, *88*, 1195−1201.

(12) Wu, H.; Wang, Y.; Qiao, X.; Wang, D.; Yang, X.; Li, H. Pyrrolo[3,2-*b*]pyrrole-Based Quinoidal Compounds For High Performance n-Channel Organic Field-Effect Transistor. *Chem. Mater.* **2018**, *30*, 6992−6997. Zhao, B.; Xu, Y.; Liu, S.; Li, C.; Fu, N.; Wang, L. Non-Fullerene Receptor Material Based on Tetrarylpyrrole Nuclear and Its Application in Organic Solar Cell Device. CN 108,912,125 A, 2018.

(13) Wang, J.; Chai, Z.; Liu, S.; Fang, M.; Chang, K.; Han, M.; Hong, L.; Han, H.; Li, Q.; Li, Z. Organic Dyes Based on Tetraaryl-1,4-dihydropyrrolo[3,2-*b*]pyrroles for Photovoltaic and Photocatalysis Applications with the Suppressed Electron Recombination. *Chem.-Eur. J.* **2018**, *24*, 18032−18042.

(14) Peng, Z.; Feng, X.; Tong, B.; Chen, D.; Shi, J.; Zhi, J.; Dong, Y. The selective detection of chloroform using an organic molecule with aggregation-induced emission properties in the solid state as a fluorescent sensor. *Sens. Actuators, B* **2016**, *232*, 264−268.

(15) Domínguez, R.; Montcada, N. F.; de la Cruz, P.; Palomares, E.; Langa, F. Pyrrolo[3,2-*b*]pyrrole as the Central Core of the Electron Donor for Solution-Processed Organic Solar Cells. *ChemPluschem* **2017**, *82*, 1096−1104.

(16) Zhou, Y.; Zhang, M.; Ye, J.; Liu, H.; Wang, K.; Yuan, Y.; Du, Y.-Q.; Zhang, C.; Zheng, C.-J.; Zhang, X.-H. Efficient Solution-Processed Red Organic Light-Emitting Diode Based on an Electron-Donating

Building Block of Pyrrolo[3,2-*b*]pyrrole. *Org. Electron.* **2019**, *65*, 110−115.
(17) Balasubramanyam, R. K. C.; Kumar, R.; Ippolito, S. J.; Bhargava, S. K.; Periasamy, S. R.; Narayan, R.; Basak, P. Quadrupolar (A-π-D-π-A) Tetra-Aryl 1,4-Dihydropyrrolo[3,2-*b*]Pyrroles as Single Molecular Resistive Memory Devices: Substituent Triggered Amphoteric Redox Performance and Electrical Bistability. *J. Phys. Chem. C* **2016**, *120*, 11313−11323.
(18) (a) Ji, Y.; Peng, Z.; Tong, B.; Shi, J.; Zhi, J.; Dong, Y. Polymorphism-dependent aggregation-induced emission of pyrrolopyrrole-based derivative and its multi-stimuli response behaviors. *Dyes Pigm.* **2017**, *139*, 664−671. (b) Li, K.; Liu, Y.; Li, Y.; Feng, Q.; Hou, H.; Tang, B. Z. 2,5-Bis(4-alkoxycarbonylphenyl)-1,4-diaryl-1,4-dihydropyrrolo[3,2-*b*]pyrrole (AAPP) AIEgens: Tunable RIR and TICT Characteristics and Their Multifunctional Applications. *Chem. Sci.* **2017**, *8*, 7258−7267. (c) Ma, Y.; Zhang, Y.; Kong, L.; Yang, J. Mechanoresponsive Material of AIE-Active 1,4-Dihydropyrrolo[3,2-b]pyrrole Luminophores Bearing Tetraphenylethylene Group with Rewritable Data Storage. *Molecules* **2018**, *23*, 3255.
(19) Hryniewicka, A.; Breczko, J.; Siemiaszko, G.; Papathanassiou, A. N.; Góra-Marek, K.; Tarach, K. A.; Brzezinski, K.; Ilnicka, A.; Terzyk, A. P.; Markiewicz, K. H.; et al.et al. Three-dimensional organization of pyrrolo[3,2-b]pyrrole-based triazine framework using nano structural spherical carbon: enhancing electrochemical performance of materials for supercapacitors. *Sci. Rep.* **2023**, *13*, 10737.
(20) Balasubramanyam, R. K. C.; Kandjani, A. E.; Harrison, C. J.; Rashid, S. S. A. A. H.; Sabri, Y. M.; Bhargava, S. K.; Narayan, R.; Basak, P.; Ippolito, S. J. 1,4-Dihydropyrrolo[3,2-*b*]pyrroles as a Single Component Photoactive Layer: A New Paradigm for Broadband Detection. *ACS Appl. Mater. Interfaces* **2017**, *9*, 27875−27882.
(21) Hawes, C. S.; Ó Máille, G. M.; Byrne, K.; Schmitt, W.; Gunnlaugsson, T. Tetraarylpyrrolo[3,2- b]pyrroles as versatile and responsive fluorescent linkers in metal−organic frameworks. *Dalton Trans.* **2018**, *47*, 10080−10092.
(22) Duan, L.-s.; Wu, Q.-p.; Xu, Y.-y.; Wang, H.; Sun, Z.; Chen, Y.; Xue, S. One-pot synthesis of tetraarylpyrrolo[3,2-*b*]pyrrole dopant-free hole-transport materials for inverted perovskite solar cells. *Chin. J. Chem. Phys.* **2021**, *34*, 217−226.
(23) (a) Clark, J. C.; Kusy, D.; Vakuliuk, O.; Krzeszewski, M.; Kochanowski, K. J.; Koszarna, B. K.; O'Mari, O.; Jacquemin, D.; Gryko, D. T.; Vullev, V. I. The magic of biaryl linkers: the electronic coupling through them defines the propensity for excited-state symmetry breaking in quadrupolar acceptor−donor−acceptor fluorophores. *Chem. Sci.* **2023**, *14*, 13537−13550. (b) Banasiewicz, M.; Stężycki, R.; Kumar, G. D.; Krzeszewski, M.; Tasior, M.; Koszarna, B.; Janiga, A.; Vakuliuk, O.; Sadowski, B.; Gryko, D. T.; Jacquemin, D. Electronic Communication in Pyrrolo[3,2-b]pyrroles Possessing Sterically Hindered Aromatic Substituents. *Eur. J. Org. Chem.* **2019**, *2019*, 5247−5253.
(24) (a) Tasior, M.; Chotkowski, M.; Gryko, D. T. Extension of Pyrrolopyrrole π-System: Approach to Constructing Hexacyclic Nitrogen-Containing Aromatic Systems. *Org. Lett.* **2015**, *17*, 6106−6109. (b) Krzeszewski, M.; Dobrzycki, Ł.; Sobolewski, A. L.; Cyrański, M. K.; Gryko, D. T. Saddle-shaped aza-nanographene with multiple odd-membered rings. *Chem. Sci.* **2023**, *14*, 2353−2360.
(25) (a) Tasior, M.; Vakuliuk, O.; Koga, D.; Koszarna, B.; Górski, K.; Grzybowski, M.; Kielesiński, Ł.; Krzeszewski, M.; Gryko, D. T. Method for the Large-Scale Synthesis of Multifunctional 1,4-Dihydropyrrolo[3,2-*b*]pyrroles. *J. Org. Chem.* **2020**, *85*, 13529−13543. (b) Tasior, M.; Koszarna, B.; Young, D. C.; Bernard, B.; Jacquemin, D.; Gryko, D.; Gryko, D. T. Fe(III)-Catalyzed Synthesis of Pyrrolo[3,2-b]pyrroles: Formation of New Dyes and Photophysical Studies. *Org. Chem. Front.* **2019**, *6*, 2939−2948.
(26) (a) Neochoritis, C. G.; Zhao, T.; Dömling, A. Tetrazoles via Multicomponent Reactions. *Chem. Rev.* **2019**, *119*, 1970−2042. (b) Benson, F. R. The chemistry of the tetrazoles. *Chem. Rev.* **1947**, *41*, 1−61.
(27) Frija, L. M. T.; Ismael, A.; Cristiano, M. L. S. Photochemical Transformations of Tetrazole Derivatives: Applications in Organic Synthesis. *Molecules* **2010**, *15*, 3757−3774.
(28) (a) Dhiman, N.; Kaur, K.; Jaitak, V. Tetrazoles as anticancer agents: A review on synthetic strategies, mechanism of action and SAR studies. *Bioorg. Med. Chem.* **2020**, *28*, 115599−115621. (b) Jin, S. C. Y.; Xia, H.; Wang, K.; Liu, Y.; Zhang, Q. Synthesis of fused tetrazolo[1,5-*b*]pyridazine-based energetic compounds. *Energy Mater. Front.* **2020**, *1*, 16−25.
(29) (a) Ponnuvel, K.; Padmini, V.; Sribalan, R. A new tetrazole based turn-on fluorescence chemosensor for Zn^{2+} ions and its application in bioimaging. *Sens. Actuators, B* **2016**, *222*, 605−611. (b) Hata, T.; Hayashi, Y.; Hasegawa, Y.; Iwai, M.; Ishii, A.; Hasegawa, M.; Shigeta, M.; Urabe, H. Preparation of Tetrazole-fused π-Conjugated Molecules and Their Fluorescence Behavior. *Chem. Lett.* **2019**, *48*, 662−665. (c) Arslan, B. S.; Derin, Y.; Mısır, B. A.; Kaya, S.; Şişman, İ.; Tutar, A.; Nebioğlu, M. Effect of electron donors on the photophysical and theoretical properties of BODIPY dyes based on tetrazolo[1,5-*a*]quinoline. *J. Mol. Struct.* **2022**, *1267*, 133608−133618. (d) West, A.-K.; Kaylor, L. J.; Subir, M.; Rayat, S. Synthesis, photophysical and nonlinear optical properties of push−pull tetrazoles. *RSC Adv.* **2022**, *12*, 22331−22341. (e) Derin, Y.; Arslan, B. S.; Mısır, B. A.; Şişman, İ.; Nebioğlu, M.; Tutar, A. Synthesis and photophysical investigation of AIEgen dyes bearing quinoline and BODIPY scaffolds. *Chem. Heterocycl. Compd.* **2020**, *56*, 1542−1547.
(30) (a) Meth-Cohn, O.; Narine, B.; Tarnowski, B. A. A versatile new synthesis of quinolines and related fused pyridines, Part 5. The synthesis of 2-chloroquinoline-3-carbaldehydes. *J. Chem. Soc., Perkin Trans.* **1981**, *1*, 1520−1530. (b) Meth-Cohn, O.; Narine, B. A versatile new synthesis of quinolines, thienopyridines and related fused pyridines. *Tetrahedron Lett.* **1978**, *19*, 2045−2048.
(31) (a) Kategaonkar, A. H.; Pokalwar, R. U.; Sonar, S. S.; Gawali, V. U.; Shingate, B. B.; Shingare, M. S. Synthesis, in vitro antibacterial and antifungal evaluations of new α-hydroxyphosphonate and new α-acetoxyphosphonate derivatives of tetrazolo [1,5-*a*] quinoline. *Eur. J. Med. Chem.* **2010**, *45*, 1128−1132. (b) Barad, H. A.; Sutariya, T. R.; Brahmbhatt, G. C.; Parmar, N. J.; Lagunes, I.; Padrón, J. M.; Murumkar, P.; Sharma, M. K.; Yadav, M. R. A catalyst- and solvent-free multicomponent synthesis and docking study of some new antiproliferative N5-allyl-quinolylpyrido[2,3-b][1,4]benzodiazepinone precursors. *New J. Chem.* **2016**, *40* (6), 4931−4939.
(32) Valeur, B.; Berberan-Santos, M. N. *Molecular Fluorescence: principles and Applications*, 2nd ed.; Wiley-VCH: Weinheim, 2012.
(33) Stark, C. W.; Rammo, M.; Trummal, A.; Uudsemaa, M.; Pahapill, J.; Sildoja, M.-M.; Tshepelevitsh, S.; Leito, I.; Young, D. C.; Szymański, B.; et al.et al. On-off-on Control of Molecular Inversion Symmetry via Multi-stage Protonation: Elucidating Vibronic Laporte Rule. *Angew. Chem., Int. Ed.* **2022**, *61*, No. e202212581.
(34) (a) Li, Q.; Huang, J.; Zhong, A.; Zhong, C.; Peng, M.; Liu, J.; Pei, Z.; Huang, Z.; Qin, J.; Li, Z. *N*-Arylpyrrole-Based Chromophores of Donor-π-Donor Type Displaying High Two-Photon Absorption. *J. Phys. Chem. B* **2011**, *115*, 4279−4285. (b) Abbotto, A.; Beverina, L.; Bozio, R.; Facchetti, A.; Ferrante, C.; Pagani, G. A.; Pedron, D.; Signorini, R. Novel Heterocycle-Based Two-Photon Absorbing Dyes. *Org. Lett.* **2002**, *4* (9), 1495.
(35) Gaussian 16, Revision A.03 , Frisch, M. J.; Trucks, G. W.; Schlegel, H. B.; Scuseria, G. E.; Robb, M. A.; Cheeseman, J. R.; Scalmani, G.; Barone, V.; Petersson, G. A.; Nakatsuji, H.; Li, X.; Caricato, M.; Marenich, A. V.; Bloino, J.; Janesko, B. G.; Gomperts, R.; Mennucci, B.; Hratchian, H. P.; Ortiz, J. V.; Izmaylov, A. F.; Sonnenberg, J. L.; Williams-Young, D.; Ding, F.; Lipparini, F.; Egidi, F.; Goings, J.; Peng, B.; Petrone, A.; Henderson, T.; Ranasinghe, D.; Zakrzewski, V. G.; Gao, J.; Rega, N.; Zheng, G.; Liang, W.; Hada, M.; Ehara, M.; Toyota, K.; Fukuda, R.; Hasegawa, J.; Ishida, M.; Nakajima, T.; Honda, Y.; Kitao, O.; Nakai, H.; Vreven, T.; Throssell, K.; Montgomery, J. A.; Peralta, J. E., Jr.; Ogliaro, F.; Bearpark, M. J.; Heyd, J. J.; Brothers, E. N.; Kudin, K. N.; Staroverov, V. N.; Keith, T. A.; Kobayashi, R.; Normand, J.; Raghavachari, K.;

https://doi.org/10.1021/acs.joc.3c02916
J. Org. Chem. 2024, 89, 4657−4672

Rendell, A. P.; Burant, J. C.; Iyengar, S. S.; Tomasi, J.; Cossi, M.; Millam, J. M.; Klene, M.; Adamo, C.; Cammi, R.; Ochterski, J. W.; Martin, R. L.; Morokuma, K.; Farkas, O.; Foresman, J. B.; Fox, D. J. *Gaussian 16, Revision A.03*; Gaussian Inc., Wallingford CT, 2016.

(36) Neese, F. Software update: the ORCA program system, version 4.0. *WIREs Comput. Mol. Sci.* **2018**, *8*, No. e1327.

(37) (a) Meth-Cohn, O.; Narine, B.; Tarnowski, B. A versatile new synthesis of quinolines and related fused pyridines. Part II. *Tetrahedron Lett.* **1979**, *20*, 3111−3114. (b) Meth-Cohn, O.; Narine, B.; Tarnowski, B. A versatile new synthesis of quinolines and related fused pyridines. Part 7. The conversion of acetamidothiophens into thienopyridines. *J. Chem. Soc., Perkin Trans.* **1981**, *1*, 1531−1536.

(38) Sonar, S. S.; Sadaphal, S. A.; Pokalwar, R. U.; Shingate, B. B.; Shingare, M. S. Synthesis and antibacterial screening of new 4-((5-(difluoromethoxy)-1*H*-benzo[d]imidazol-2-ylthio)methyl)tetrazolo-[1,5-a]quinoline derivatives. *J. Heterocycl. Chem.* **2010**, *47*, 441−445.

(39) Izawa, T.; Miyazaki, E.; Takimiya, K. Solution-Processible Organic Semiconductors Based on Selenophene-Containing Heteroarenes, 2,7-Dialkyl[1]benzoselenopheno[3,2-*b*][1]benzoselenophenes (C_n-BSBSs): Syntheses, Properties, Molecular Arrangements, and Field-Effect Transistor Characteristics. *Chem. Mater.* **2009**, *21*, 903−912.

(40) De Ridder, R.; Martin, R. H. Synthèses dans le Domaine des Composés Polycycliques Aromatiques. XVIII—1,2,3,4,5,6-Tribenzofluorène (Ou Tribenzo [a,c,g] Flourène) Et 1,2,3,4,5,6,7,8-Tétrabenzofluoréne (ou Tétrabenzo [a,c,g,i] Flourène). *Bull. Soc. Chim. Belg.* **1960**, *69*, 534−548.

https://doi.org/10.1021/acs.joc.3c02916
J. Org. Chem. 2024, 89, 4657−4672